

Journal of Visualized Experiments

Autofluorescence Imaging to Evaluate Cellular Metabolism

--Manuscript Draft--

Article Type:	Invited Methods Collection - JoVE Produced Video
Manuscript Number:	JoVE63282R2
Full Title:	Autofluorescence Imaging to Evaluate Cellular Metabolism
Corresponding Author:	Alexandra Walsh UNITED STATES
Corresponding Author's Institution:	
Corresponding Author E-Mail:	walshaj@tamu.edu
Order of Authors:	Alexandra Walsh Anna Theodossiou Linghao Hu Nianchao Wang Uyen Nguyen
Additional Information:	
Question	Response
Please specify the section of the submitted manuscript.	Bioengineering
Please indicate whether this article will be Standard Access or Open Access.	Standard Access (\$1400)
Please indicate the city, state/province, and country where this article will be filmed . Please do not use abbreviations.	College Station, Texas United States
Please confirm that you have read and agree to the terms and conditions of the author license agreement that applies below:	I agree to the Author License Agreement
Please confirm that you have read and agree to the terms and conditions of the video release that applies below:	I agree to the Video Release
Please provide any comments to the journal here.	The supplementary files are going to be linked to a GitHub page so it is easily accessible to the reader. The link is provided in the protocol.

TITLE:

Autofluorescence Imaging to Evaluate Cellular Metabolism

AUTHORS AND AFFILIATIONS:

Anna Theodossiou, Linghao Hu, Nianchao Wang, Uyen Nguyen, Alex J. Walsh

Department of Biomedical Engineering, Texas A&M University-College Station, TX 77843, USA

Email addresses of co-authors:

Anna Theodossiou (annatheodossiou@tamu.edu)

Linghao Hu (hulinghao@tamu.edu)

Nianchao Wang (nwang27@tamu.edu)

Uyen Nguyen (uyenguyen98@tamu.edu)

Corresponding author:

Alex J. Walsh (walshaj@tamu.edu)

KEYWORDS:

FLIM, Metabolism, NAD(P)H, FAD, Fluorescence, Microscopy

SUMMARY:

This protocol describes fluorescence imaging and analysis of the endogenous metabolic coenzymes, reduced nicotinamide adenine (phosphate) dinucleotide (NAD(P)H), and oxidized flavin adenine dinucleotide (FAD). Autofluorescence imaging of NAD(P)H and FAD provides a label-free, nondestructive method to assess cellular metabolism.

ABSTRACT:

Cellular metabolism is the process by which cells generate energy, and many diseases, including cancer, are characterized by abnormal metabolism. Reduced nicotinamide adenine (phosphate) dinucleotide (NAD(P)H) and oxidized flavin adenine dinucleotide (FAD) are coenzymes of metabolic reactions. NAD(P)H and FAD exhibit autofluorescence and can be spectrally isolated by excitation and emission wavelengths. Both coenzymes, NAD(P)H and FAD, can exist in either a free or protein-bound configuration, each of which has a distinct fluorescence lifetime—the time for which the fluorophore remains in the excited state. Fluorescence lifetime imaging (FLIM) allows quantification of the fluorescence intensity and lifetimes of NAD(P)H and FAD for label-free analysis of cellular metabolism. Fluorescence intensity and lifetime microscopes can be optimized for imaging NAD(P)H and FAD by selecting the appropriate excitation and emission wavelengths. Metabolic perturbations by cyanide verify autofluorescence imaging protocols to detect metabolic changes within cells. This article will demonstrate the technique of autofluorescence imaging of NAD(P)H and FAD for measuring cellular metabolism.

INTRODUCTION:

Metabolism is the cellular process of producing energy. Cellular metabolism encompasses multiple pathways, including glycolysis, oxidative phosphorylation, and glutaminolysis. Healthy

cells use these metabolic pathways to generate energy for proliferation and function, such as the production of cytokines by immune cells. Many diseases, including metabolic disorders, cancer, and neurodegeneration, are characterized by altered cellular metabolism¹. For example, some cancer cell types have elevated rates of glycolysis, even in the presence of oxygen, to generate molecules for the synthesis of nucleic acids, proteins, and lipids^{2,3}. This phenomenon, known as the Warburg effect, is a hallmark of many cancer types, including breast cancer, lung cancer, and glioblastomas⁴. Because of the alterations of cellular metabolism associated with cancer progression, cellular metabolism can be a surrogate biomarker for drug response^{5,6}. Moreover, understanding drug efficacy at a cellular level is crucial as cell heterogeneity can lead to differing drug responses in individuals^{7,8}.

Technologies that identify and quantify changes in cellular metabolism are essential for studies of cancer and drug response. Chemical and protein analyses are used to evaluate the metabolism of cells or tissues but lack single-cell resolution and spatial information. Metabolic plate reader-based assays can measure pH and oxygen consumption in the sample over time and the subsequent metabolic perturbation by chemicals. The pH can be used to calculate the extracellular acidification rate (ECAR), which provides an insight into the glycolytic activity of the cells⁹. Whole-body imaging methods, including 2-[fluorine-18] fluoro-D-glucose positron emission tomography (FDG PET) and magnetic resonance spectroscopy (MRS), are noninvasive imaging modalities used clinically to identify tumor recurrence and drug efficacy through metabolic measurements¹⁰⁻¹⁴.

FDG-PET images the tissue uptake of FDG, a radiolabeled glucose analog. Increased uptake of FDG-PET by tumors relative to surrounding tissue is due to the Warburg effect^{12,13}. MRS images common nuclei of molecules used for metabolism, such as ¹³C and ³¹P, and can obtain dynamic information about how metabolism changes in response to stimuli, such as exercise or eating¹⁴. Although FDG-PET and MRS can be used clinically, these technologies lack the spatial resolution to resolve intratumoral heterogeneity. Likewise, oxygen consumption measurements are made on a bulk population of cells. Autofluorescence imaging overcomes the spatial resolution obstacle of these technologies and provides a noninvasive method of quantifying cellular metabolism.

[Insert Figure 1 here]

Reduced nicotinamide adenine (phosphate) dinucleotide (NAD(P)H) and oxidized flavin adenine dinucleotide (FAD) are coenzymes of metabolic reactions, including glycolysis, oxidative phosphorylation, and glutaminolysis (**Figure 1**). Both NAD(P)H and FAD are autofluorescent and provide endogenous contrast for fluorescence imaging^{1,15}. NADPH has similar fluorescent properties to NADH. Because of this, NAD(P)H is often used to represent the combined signal of NADH and NADPH^{2,16}.

Fluorescence lifetime imaging (FLIM) quantifies the fluorescence lifetime or the time for which a fluorophore is in the excited state. Fluorescence lifetimes are responsive to the microenvironment of the fluorophores and provide information about cellular metabolism¹⁷. NAD(P)H and FAD can exist within cells in either protein-bound or free conformations, each of

which has a different lifetime. Free NAD(P)H has a shorter lifetime than protein-bound NAD(P)H; conversely, free FAD has a longer lifetime than bound FAD^{18,19}. The lifetimes and lifetime component weights can be quantified from fluorescence lifetime decay data through Eq. (1)²⁰:

$$I(t) = \alpha_1 e^{-t/\tau_1} + \alpha_2 e^{-t/\tau_2} + C \quad (1)$$

Eq (1) represents the normalized fluorescence intensity as a function of time. The α_1 and α_2 in this equation represent the proportional components of short and long lifetimes ($\alpha_1 + \alpha_2 = 1$), respectively, τ_1 and τ_2 represent the short and long lifetimes, respectively, and C accounts for background light^{7,20}. The amplitude-weighted lifetime, represented here as τ_m , is calculated using Eq. (2).

$$\tau_m = \alpha_1 \tau_1 + \alpha_2 \tau_2 \quad (2)$$

A mean lifetime can be computed by averaging “t” over the intensity decay of the fluorophore, which for a two-exponential decay is shown by Eq. (3)^{17,21}.

$$\tau_m^* = (\alpha_1 \tau_1^2 + \alpha_2 \tau_2^2) / (\alpha_1 \tau_1 + \alpha_2 \tau_2) \quad (3)$$

A fluorescence intensity image can be computed from the lifetime image by integrating the fluorescence lifetime decay. Autofluorescence imaging is a nondestructive and label-free method that can be used to characterize the metabolism of live cells at a subcellular resolution. The optical redox ratio provides an optical analog metric of the chemical redox state of the cell and is calculated as the ratio of NAD(P)H and FAD intensities. Although the formula for calculating the optical redox ratio is not standardized²²⁻²⁵, it is defined here as the intensity of FAD over the combined intensities of NAD(P)H and FAD. This definition is used because the summed intensity in the denominator normalizes the metric between 0 and 1, and the expected result of the cyanide inhibition is a decrease in the redox ratio. The fluorescence lifetimes of free NAD(P)H and FAD provide insight into changes in the metabolic solvent microenvironment, including pH, temperature, proximity to oxygen, and osmolarity¹⁷.

Changes in the fluorescence lifetime of the bound fractions of NAD(P)H and FAD can indicate metabolic pathway utilization and substrate-specific metabolism²⁶. Component weights can be interpreted for changes in the free to the bound fraction of the coenzymes^{18,19}. Altogether, these quantitative autofluorescence lifetime metrics allow the analysis of cellular metabolism, and autofluorescence imaging has been used for identifying neoplasms from normal tissues^{27,28}, characterizing stem cells^{29,30}, evaluating immune cell function³¹⁻³⁵, gauging neurological activity³⁶⁻³⁸, and understanding drug efficacy in cancer types such as breast cancer and head and neck cancer^{21,39-42}. High-resolution autofluorescence imaging can be combined with image segmentation for single-cell analysis and quantification of intrapopulation heterogeneity⁴³⁻⁴⁷.

NAD(P)H and FAD can be imaged on single-photon or multiphoton fluorescence microscopes configured for intensity or lifetime imaging. For single-photon microscopes, NAD(P)H and FAD are typically excited at wavelengths of 375–405 nm and 488 nm, respectively, due to common

laser sources at these wavelengths⁴⁸. In two-photon fluorescence excitation, NAD(P)H and FAD will excite at wavelengths of approximately 700 to 750 nm and 700 to 900 nm, respectively^{15,49}. Once the fluorophores are excited, NAD(P)H and FAD emit photons at wavelengths between ~410 nm to ~490 nm and ~510 nm to ~640 nm, respectively¹⁵. The NAD(P)H and FAD maxima emission wavelengths are approximately 450 nm and 535 nm, respectively⁴⁸.

Because of their different excitation and emission wavelengths, the fluorescence of the two metabolic coenzymes can be spectrally isolated. An understanding of the spectral characteristics of NAD(P)H and FAD is necessary for the design and optimization of autofluorescence imaging protocols. Cyanide is an electron complex chain (ETC) complex IV inhibitor. The effects of cyanide on cellular metabolism and the autofluorescence intensities and lifetimes of NAD(P)H and FAD within cells are well characterized^{27,40}. Therefore, a cyanide perturbation experiment is an effective means of validating NAD(P)H and FAD imaging protocols. A successful cyanide experiment provides confidence that the NAD(P)H and FAD imaging protocol can be used to assess the metabolism of unknown groups or perturbations.

PROTOCOL:

1. Cell plating for imaging

1.1. Aspirate the medium from an 80–90% confluent T-75 flask of MCF-7 cells, rinse the cells with 10 mL of sterile phosphate-buffered saline (PBS), and add 2 mL of 0.25% trypsin (1x) to detach the cells from the flask bottom.

1.2. Incubate the flask at 37 °C for ~4 min. Check the cells under the microscope to confirm detachment.

1.3. Immediately add 8 mL of culture medium to de-activate the trypsin.

1.4. Collect the cells in a conical tube (15 mL or 50 mL). Count the cells using a hemocytometer.

1.5. Centrifuge the cells $200 \times g$ for 5 min.

1.6. Once centrifuged, aspirate the supernatant. Resuspend the pellet of cells in 1 mL of culture medium, and seed 4×10^5 cells onto a 35 mm glass-bottom imaging dish (or the appropriate sample holder for the microscope being used).

1.7. Add 2 mL of culture medium to the imaging dish to maintain cell metabolism.

1.8. Incubate the cells at 37 °C with 5% CO₂ for 24–48 h prior to imaging for the cells to adhere and reach the logarithmic growth phase.

NOTE: The growth phase was determined by prior experience with these cells and confirmed with

the cell datasheet.

2. Multiphoton FLIM imaging of NAD(P)H and FAD

2.1. Turn on all components of the multiphoton fluorescence lifetime microscope, including the microscope, the laser source, and the detectors being used.

2.2. Sample placement

2.2.1. Turn on the brightfield lamp. Ensure that light is going into the eyepiece. Choose an objective, usually 20x, 40x, or 100x for cell imaging. Apply 1 drop of the appropriate immersion medium on top of the objective [skip if using an air objective].

2.2.2. Move the objective down to properly place the sample without touching the objective. Place the glass-bottom dish onto the sample holder on the microscope stage. Ensure that the specimen is secure and will not move during imaging.

2.2.3. Center the specimen with the objective using the X-Y stage control. Once this is done, look into the eyepiece and move the objective up to focus on the cells.

2.2.4. If the microscope is within an enclosure, close the lightbox door. Open the image acquisition software, click on the **Multiphoton Imaging** tab, and set the following multiphoton imaging parameters: image size = 256 x 256 pixels; pixel dwell time = 4–25 μ s; total image acquisition time = ~60 s; optimized detector gain for single-photon counting = 85% (specific to the system being used).

2.3. Imaging of Instrument Response Function (IRF) and Fluorescent Lifetime Standard

2.3.1. Place urea crystals on a glass-bottom dish and secure the dish lid with tape or parafilm.

NOTE: Urea crystals remain stable at room temperature for months.

2.3.2. Image the urea crystals.

2.3.2.1. Place the urea dish on the microscope stage and focus on a urea crystal.

2.3.2.2. Set the wavelength of the excitation laser to 900 nm.

2.3.2.3. Use an emission filter that captures 450 nm wavelengths.

2.3.2.4. Obtain a fluorescence lifetime image of the urea crystal with laser power at the sample <1 mW and use the recommended imaging parameters mentioned in step 2.2.4.

2.3.3. Image the Yellow-green (YG) beads as a fluorescence lifetime standard.

2.3.3.1. Create a YG bead slide by diluting the YG bead solution 1:1,000 in sterile water. Place a small volume (~30 μ L) onto a slide or glass-bottom dish. Cover with a coverslip and seal the edges of the coverslip with clear nail polish.

2.3.3.2. Place the YG bead slide on the microscope stage with the coverslip side of the slide towards the objective.

2.3.3.3. Set the wavelength of the excitation laser to 890 nm

2.3.3.4. Use an emission filter that captures ~500–600 nm wavelengths.

2.3.3.5. Obtain a fluorescence lifetime image of the YG bead using a laser power at the sample <1 mW and the recommended image parameters [step 2.2.4].

2.3.3.6. Check the lifetime of the bead using the IRF of the urea. If the lifetime is not ~2.1 ns, check whether the bead is in contact with another bead contributing to fluorescence quenching, the bead solution has dried, the bead is out of focus, IRF is not accurate, or the shift between IRF and fluorescence decay is not optimized [see step 4.2.4].

NOTE: The lifetime of ~2.1 ns is stable over time.

2.4. NAD(P)H imaging

2.4.1. Place the glass-bottom dish with the cells on the microscope stage and focus on the cells.

NOTE: It is recommended that the cells be placed in an environmental chamber to maintain heat, humidity, and CO₂ levels during image acquisition, as these parameters can influence cellular metabolism.

2.4.2. Adjust the gain of the detector to the optimal value for FLIM. Additionally, change to the desired dwell time—a parameter indicating the time the laser spends at each pixel of the specimen.

NOTE: These parameters should stay the SAME throughout the remainder of the procedure. This is to ensure consistency in laser illumination and detector settings to ensure the validity of the intensity-based measurements, which are dependent on laser power, scan parameters, and detector gain. There is an optimized detector gain for operating detectors in single-photon counting mode; the value is 85% for the system referenced.

2.4.3. Set the multiphoton laser to 750 nm. Ensure that the power control for the laser is set at zero initially so that the cells are not damaged upon opening the shutter on the laser.

NOTE: Excitation at 750 nm is recommended for NAD(P)H, although it has broad absorption at

700–750 nm. Excitation at 890 nm is recommended for FAD, although it has broad absorption at 700–900 nm.

2.4.4. Set or select an emission filter to collect emission wavelengths at ~400–500 nm.

2.4.5. Begin imaging in a **focusing** or **live-view** manner to optimize the image settings.

NOTE: The laser is now operating. Do not open the microscope enclosure at this point. Wear appropriate personal protective equipment.

2.4.6. Slowly increase the laser power to ~ 3–8 mW at the sample while also ensuring the cells are in focus. Once adjusted, record the maximum power used. Use this power setting for the imaging on other segments of the Petri dish for NAD(P)H imaging.

NOTE: It is important to measure the laser power at the sample or a pick-off window and not rely on the pockels cell voltage as the pockels cells are not stable. Often laser power is monitored during imaging with a pick-off window instead of at the sample. Using a second power meter at the objective, the relationship between the power at the pick-off window and the power at the sample can be used to estimate the approximate power at the sample from the pick-off window measurements.

2.4.7. Collect an NAD(P)H FLIM image with an image integration time of 60 s.

2.4.8. Check that the image has sufficient photons (peak of ~100 photons for a cytoplasm pixel) within the fluorescence lifetime decay curve. If the number of photons is too low, increase the laser power or duration of image acquisition.

NOTE: The minimum peak number of photons within the fluorescence exponential decay is dependent on system parameters, including temporal resolution, IRF, and background noise.

2.5. FAD imaging

2.5.1. Set the multiphoton laser to 890 nm and wait for it to mode-lock at the new wavelength. Ensure that the power control for the laser is set at zero initially so that the cells are not damaged upon opening the shutter on the laser.

NOTE: Do not move the stage or objective focus when conducting this step. The FAD field of view (FOV) should directly match NAD(P)H FOV for this image.

2.5.2. Set or select an emission filter to collect emission wavelengths at ~500–600 nm.

2.5.3. Begin imaging in a **focusing** or **live-view** manner to optimize the image settings.

NOTE: The laser is now operating. Do not open the microscope enclosure at this point.

2.5.4. Slowly increase the laser power to ~5–10 mW at the sample and record the maximum power used. Use this as the power setting for the imaging on other segments of the Petri dish for FAD imaging.

2.5.5. Collect an FAD FLIM image with an image integration time of 60 s.

2.5.6. Check that the image has sufficient photons (peak of ~100 photons for a cytoplasm pixel) within the fluorescence lifetime decay curve. If the number of photons is too low, increase the laser power or duration of image acquisition.

NOTE: The minimum peak number of photons within the fluorescence exponential decay is dependent on system parameters, including temporal resolution, IRF, and background noise.

2.6. Repeat steps 2.4–2.5 at an additional four to five FOVs. Ensure that each image is spaced at least 2 FOVs away from the imaged locations.

3. Cyanide experiment preparation

3.1. Dissolve 130.24 mg of sodium cyanide in 25 mL of PBS to make an 80 mM (20x) sodium cyanide solution.

NOTE: Cyanide is toxic. Wear appropriate personal protective equipment.

3.2. Aspirate 100 μ L of culture medium from the dish. Replace this with 100 μ L of sodium cyanide solution to obtain a 4 mM concentration of cyanide in the dish.

3.3. Put the cells in an incubator for 5 min to allow the cells to react with the cyanide solution.

3.4. Repeat steps 2.4–2.6 to acquire NAD(P)H and FAD images of the cells after cyanide exposure.

NOTE: Prolonged exposure to cyanide will kill the cells. Postcyanide images are acquired within 30 min of the cyanide addition.

4. FLIM image analysis

4.1. Open the FLIM lifetime analysis software.

4.1.1. Open the urea image to acquire the measured IRF.

4.1.2. Import the urea image. Select a **point on the image** of the urea crystal to be used for image analysis. Increase the **spatial bin value** to integrate FLIM data from multiple pixels to 1 or

higher for a **decay peak > 100 photons** by changing the **Bin** variable located on the main software interface.

4.1.3. Save the data as an **IRF**.

4.1.3.1. In the referenced software, click the dropdown menu titled **IRF**, select **Copy from Decay Data**. After this, click **Copy to Clipboard** to be utilized in the image analysis of the image taken during the experiment.

4.2. Image analysis of NAD(P)H and FAD lifetime images

4.2.1. Import the image file into fluorescence lifetime analysis software.

4.2.2. Improve image visualization to see the cells and subcellular compartments by changing the intensity and contrast if needed.

4.2.2.1. Click the **Options** dropdown menu and select **Intensity**. Here, change the intensity and contrast as desired and click **Ok**.

4.2.3. Import the IRF from the urea image.

4.2.3.1. Click the **IRF** dropdown menu and select **Paste from Clipboard**.

4.2.4. Set **Multiexponential Decay** parameters⁵⁰.

4.2.4.1. Set a threshold value to evaluate decays for cytoplasm pixels.

NOTE: Here, a value of 50 was used. The value was selected by comparing the fluorescence peak values of several representative background and nucleus pixels with the peak value of several cytoplasm pixels. A value between the nucleus pixels and cytoplasm pixels was selected for the threshold.

4.2.5. Check that the Shift value aligns the IRF relative to the rising edge of the fluorescence. Adjust the shift if needed to a value that minimizes the Chi-squared value.

4.2.6. Increase the spatial bin so that cytoplasm pixels have fluorescence peak values at or above 100.

NOTE: Increasing the spatial bin will lead to decreased spatial resolution.

4.2.7. Compute fluorescence lifetimes for all pixels in the image.

4.2.7.1. In the referenced program, click the **Calculate** dropdown menu | **Decay Matrix**.

NOTE: Success is indicated with an image false-colored to the amplitude-weighted fluorescence lifetime.

4.2.8. Save the fluorescence lifetime data.

4.2.8.1. Click the **File** dropdown menu | **Export**. Choose the desired parameters for analysis and click **Ok**. Save the image.

4.2.8.2. Select the **Color** button from the **Options** dropdown menu to adjust the fluorescence lifetime metric displayed, the **color configuration** to **B-G-R**, and set the specific color bar minimum and maximum values to adjust the color scale of the fluorescence lifetime image.

[Insert Figure 2 here]

4.3. Cell segmentation

NOTE: The protocol described here uses an image analysis software⁵¹. Representative MCF-7 images and data analysis code are provided⁵².

4.3.1. Download the **MCF7_Segmentation_Final.cpproj** file⁵².

4.3.2. Import the MCF7_Segmentation Pipeline by clicking on **File** | **Import** | **Pipeline from file**, select the file **MCF7_Segmentation_Final.cpproj**.

4.3.3. Click the **Images** module and add the NAD(P)H intensity images to be segmented.

NOTE: Images must be in.tif, .png, or .jpg format.

4.3.4. Press **Analyze Images** button on the bottom left.

NOTE: Pipeline may need optimization for images acquired on different systems. For troubleshooting, try steps 4.3.4.1–

4.3.4.1. Use the **Test** Mode for testing different parameters: Click **Start Test Mode** and run each module by clicking the **play** button next to the module name.

4.3.4.2. Click the first **IdentifyPrimaryObjects** module and adjust the **Typical diameter of objects, in pixel units (Min, Max)** to match the diameter of the cells.

NOTE: For MCF-7 cells, 10 and 40 pixels were used for the minimum and maximum, respectively.

4.3.4.3. Click the **EnhanceOrSuppressFeatures** module and adjust the **Feature size** to improve identification of the selected **Feature type**.

NOTE: A feature size of 10 pixels was used for MCF-7 cells.

4.3.4.4. Click the second **EnhanceOrSuppressFeatures** module and adjust the **Range of hole sizes** to optimize the enhancement of the nuclear regions.

NOTE: A range of 5–20 was used for MCF-7 cells.

4.3.4.5. Click the second **IdentifyPrimaryObjects** module and adjust the parameters (**Threshold strategy**, **Thresholding method**, **Threshold smoothing scale**, and **Threshold correction factor**) to optimize the identification of nuclei. Click on the ? by each parameter to identify optimal settings and apply to the **IdentifySecondaryObjects** module.

4.3.4.6. Click on the **FilterObjects** module and adjust the area shape. Select a minimum and maximum pixel of the area shape to be identified.

NOTE: For the MCF-7 cells, 100 and 500 were used for the maximum and minimum, respectively. The process of cell segmentation by identifying the nucleus and propagation to the cell boundaries is explained in detail by Walsh and Skala⁴⁷.

4.3.5. Using the cell cytoplasm masks, average the fluorescence lifetime output variables for each cell within the image.

[Insert Figure 3 here]

5. **Alternative method: Fluorescence intensity imaging**

5.1. Turn on the equipment that will be used during the experiment.

NOTE: Fluorescence intensity images can be acquired with wide-field fluorescence microscopes, confocal fluorescence microscopes, or multiphoton microscopes.

5.1.1. Ensure that the microscope to be used has an appropriate excitation source for NAD(P)H (single-photon wavelength ~370–405 nm; two-photon wavelength ~700–750 nm) and FAD (single-photon wavelength ~488 nm, two-photon wavelength ~890 nm).

5.1.2. Ensure that the microscope has a filter for the isolation of NAD(P)H emission (~400–500 nm).

NOTE: 4',6-Diamidino-2-phenylindole (DAPI) settings often work for NAD(P)H.

5.1.3. Ensure that the microscope has a filter for isolation of FAD emission (~500–600 nm).

NOTE: Green fluorescent protein (GFP) settings often work for FAD.

5.2. Prepare the microscope.

5.2.1. Turn on the brightfield lamp. Ensure that light is going into the eyepiece. Apply 1 drop of the appropriate immersion medium on top of the corresponding objective if needed.

5.2.2. Move the objective down to properly place the samples without any interference. Place the Petri dish onto the stage properly. Ensure that the specimen is secure and will not move during imaging.

NOTE: It is recommended that the cells be placed in an environmental chamber to maintain heat, humidity, and CO₂ levels during image acquisition, as these parameters can influence cellular metabolism.

5.2.3. Center the specimen with the objective. Once this is done, look into the eyepiece and move the objective until the cells appear to be in focus.

5.3. Begin intensity imaging.

5.3.1. Open up the imaging software and set the excitation and emission configuration to capture NAD(P)H by clicking the **Capture** tab in the image acquisition software and positioning the NAD(P)H excitation and emission filter in the microscope turret.

NOTE: A 357/44 excitation filter, 409 longpass dichroic, and 447/60 emission filter were used for NAD(P)H imaging.

5.3.2. Optimize the excitation illumination and detector parameters. If bleaching is an issue, reduce the illumination intensity and increase the image integration time.

NOTE: NAD(P)H is a weak signal; be aware of bleaching if too much power is used.

5.3.3. Acquire an NAD(P)H image of the desired image size. Ensure that the image is saved.

5.3.4. Set the excitation and emission configuration to capture FAD. Optimize the excitation illumination and detector parameters.

NOTE: A 458/64 excitation filter, 495 longpass dichroic, and 550/88 emission filter were used for FAD imaging.

5.3.5. Acquire an FAD image. Ensure that the image is saved.

NOTE: NAD(P)H and FAD image acquisition parameters (illumination intensity, image size, detector gain) should stay the **same** throughout the imaging experiment.

5.3.6. Repeat the process at an additional five locations, spaced at least 2 FOVs away from the imaged locations.

5.4. Image-level redox ratio data analysis

5.4.1. Open the NAD(P)H and FAD intensity images in an image processing program.

5.4.2. Set a threshold on the NAD(P)H to retain cytoplasm pixels and set background and nucleus pixels to 0.

5.4.3. Calculate the redox ratio image by evaluating the equation $FAD/(NAD(P)H+FAD)$ at each pixel using the thresholded NAD(P)H image.

5.4.4. Calculate the mean value of the non-0 pixels.

NOTE: These steps can be performed in image analysis software or coded directly with scripts.

5.5. Cell-level redox ratio analysis

5.5.1. Follow steps 4.3.1–4.3.12 to obtain a mask image of the cells within each NAD(P)H image.

5.5.2. Calculate the redox ratio image by evaluating the equation $FAD/(NAD(P)H+FAD)$ at each pixel.

5.5.3. Using the cell cytoplasm mask, average the redox ratio for all pixels for each cell within the image.

REPRESENTATIVE RESULTS:

The epithelial breast cancer cell line, MCF-7, was cultured in DMEM supplemented with 10% fetal bovine serum (FBS) and 1% penicillin–streptomycin. For fluorescence imaging, the cells were seeded at a density of 4×10^5 cells per 35 mm glass-bottom imaging dish 48 h before imaging. The cells were imaged before and after cyanide treatment using the protocols stated above. The goal of the cyanide experiment is to confirm spectral isolation of NAD(P)H and FAD fluorescence and validate the imaging system and analysis protocol for detecting metabolic changes in cells. Paired NAD(P)H and FAD fluorescence lifetime images were taken at five different locations before cyanide and five different locations after the addition of cyanide to the medium. Fluorescence lifetime parameters (optical redox ratio, NAD(P)H α_1 , NAD(P)H τ_1 , NAD(P)H τ_2 , NAD(P)H τ_m , FAD τ_1 , FAD τ_2 , FAD α_1 , FAD τ_1 , FAD τ_2 , and FAD τ_m) were calculated using the measured IRF from urea (**Figure 2**) and averaged across the pixels of the cytoplasm of each cell used for segmentation (**Figure 3**).

Multiphoton fluorescence lifetime imaging of NAD(P)H and FAD allows visualization of cell morphology and metabolism (**Figure 4**). The high resolution achieved with multiphoton microscopy allows for the identification of single cells. NAD(P)H and FAD are primarily located in the mitochondria and cytoplasm, while the nucleus, which lacks metabolic NAD(P)H and FAD, is dark in comparison^{23,53}. The lifetime images provide visualization of the amplitude-weighted

lifetimes of NAD(P)H and FAD throughout the cell and as a result of cyanide exposure (**Figure 4**).

[Insert Figure 4 here]

Cyanide inhibits complex IV of the electron transport chain, which inhibits oxidative phosphorylation^{2,15}. After cyanide exposure and prior to cell death, NAD(P)H accumulates within the mitochondria, and FAD decreases^{1,15}. Due to these well-defined changes in NAD(P)H and FAD intensity due to cyanide inhibition of metabolism, the perturbation is a standard test to verify autofluorescence imaging and analysis protocols^{2,54}. As expected, the optical redox ratio (FAD/(FAD+NAD(P)H)) of MCF-7 cells decreased after cyanide treatment (**Figure 5**, $p = 0.044$, Welch's t -test). The optical redox ratio is not a standardized formula, yet all intensity formulas have been shown to be equivalent²⁰. FAD/(NAD(P)H+FAD) was chosen to define the optical redox ratio because the combined sum of NAD(P)H and FAD in the denominator provides a normalized value between 0 and 1^{20,55}. The opposite effect—an increase in optical redox ratio—is expected for cyanide perturbations with optical redox ratios calculated with NAD(P)H in the numerator.

[Insert Figure 5 here]

The amplitude-weighted NAD(P)H lifetime (τ_m) of MCF7 cells decreased with cyanide exposure (**Figure 6A**, $p < 2.2 \times 10^{-16}$, Welch's t -test). Both the short and long lifetimes decreased for NAD(P)H (**Figure 6B,C**) but increased for NAD(P)H α_1 (**Figure 6D**). These changes in NAD(P)H fluorescence lifetimes, decrease in τ_m , increase in α_1 , and decrease in τ_2 matched published values of cyanide perturbations^{40,56}. The decrease in NAD(P)H amplitude-weighted fluorescence lifetime with cyanide exposure indicates increased quenching within the microenvironment of NAD(P)H. An increase in α_1 indicates more free NAD(P)H, as expected from the increase of NAD(P)H due to the effects of cyanide on cellular metabolism²¹.

[Insert Figure 6 here]

The amplitude-weighted FAD lifetime (τ_m) of MCF7 cells increased after cyanide exposure (**Figure 7A**, $p = 3.688 \times 10^{-12}$, Welch's t -test). Both the short and long lifetimes increased for FAD (**Figure 7B,C**) but decreased for FAD α_1 (**Figure 7D**). Changes in FAD fluorescence lifetimes, an increase in τ_m and τ_2 , and a decrease in α_1 are consistent with published FAD fluorescence lifetime data of cyanide perturbation⁵⁷. The change in lifetime values and α_1 suggest metabolic changes within the cells, including an increased amount of free FAD²¹.

[Insert Figure 7 here]

FIGURE AND TABLE LEGENDS:

Figure 1: NADH and FAD in common metabolic pathways. NADH and FAD are coenzymes used in glycolysis, the Krebs cycle, and the electron transport chain. Autofluorescence imaging of these molecules provides information about cellular metabolism.

Figure 2: Measured IRF of urea crystal. (A) Intensity image obtained from the urea. A representative pixel was chosen to create the IRF decay curve (B) for subsequent analysis of fluorescence lifetime images of cells. Abbreviation: IRF = instrument response function.

Figure 3: Identification and segmentation of individual cells. The NAD(P)H intensity image of MCF7 cells (A) obtained by integrating a fluorescence lifetime image. Cells were imaged using 750 nm excitation at 5 mW for 60 s. The x and y axes represent the pixel location of the image. (A) Individual cells were identified. The cells were masked (B) to eliminate any background noise from the data set. The nucleus was then identified (C) and projected onto the cell mask (D). The cells were then filtered (E) to remove masked areas that do not fit the size of typical cells. Scale bar = 50 μ m.

Figure 4: Representative fluorescence lifetime images of MCF7 cells before and after cyanide treatment. (A) NAD(P)H amplitude-weighted fluorescence lifetime image and (B) FAD amplitude-weighted fluorescence lifetime image before cyanide treatment. (C) NAD(P)H amplitude-weighted fluorescence lifetime image and (D) FAD amplitude-weighted fluorescence lifetime image after cyanide treatment. The amplitude-weighted fluorescence lifetime (indicated by the color bar) measures the time for which a fluorophore, in these cases NAD(P)H and FAD, is in an excited state. NAD(P)H lifetime decreases with cyanide treatment, whereas the FAD lifetime increases after cyanide treatment. NADH signal was imaged using 750 nm excitation at 5 mW for 60 s, and the FAD signal was imaged using 890 nm excitation at 7 mW for 60 s. Images acquired with a 40x water-immersion objective, numerical aperture = 1.1. Scale bar = 50 μ m.

Figure 5: Optical redox ratio of MCF7 cells decrease with cyanide treatment. The boxplots show the median and the first and third quartiles calculated from the cell data. The mean is represented by the black dot symbol, and the median is represented by the black line inside the box. The gray data points overlaid on each boxplot represent the averaged value of all the cytoplasm pixels within each cell. The control group consisted of 91 cells from five different images, and the cyanide group consisted of 95 cells from five different images. $p < 0.01$, Welch's t -test.

Figure 6: NAD(P)H fluorescence lifetime of MCF7 cells before and after cyanide treatment. The boxplots in panels A–D show the median and the first and third quartiles calculated from the cell-level data. The mean is represented by the black dot symbol, and the median is represented by the black line inside the box. The gray data points overlaid on each boxplot represent the averaged value of all the cytoplasm pixels within a cell. The control group consisted of 91 cells from five different images, and the cyanide group consisted of 95 cells from five different images. (A–D) exhibit the changes in NAD(P)H amplitude-weighted lifetime (τ_m), NAD(P)H short lifetime (τ_1), NAD(P)H long lifetime (τ_2), and NAD(P)H-proportional component of the short lifetime (α_1) due to cyanide treatment. p -values were calculated using Welch's t -test.

Figure 7: FAD fluorescence lifetime before and after cyanide treatment. The boxplots in A–D show the median, the first and third quartiles, and mean calculated from the cell-level data. The mean is represented by the black dot symbol, and the median is represented by the black line

inside the box. The gray data points overlaid on each boxplot represent the averaged value of all the cytoplasm pixels within a cell. The control group consisted of 91 cells from five different images, and the cyanide group consisted of 95 cells from five different images. (A–D) exhibit the changes in FAD amplitude-weighted lifetime (τ_m), FAD short lifetime (τ_1), FAD long lifetime (τ_2), and FAD-proportional component of the short lifetime (α_1) from cyanide treatment. p-values were calculated using Welch's *t*-test.

DISCUSSION:

Autofluorescence intensity and lifetime imaging have been widely used to assess metabolism in cells^{21,55}. FLIM is high resolution and therefore resolves single cells, which is important for cancer studies because cellular heterogeneity contributes to tumor aggression and drug resistance^{7,39,41,44–46,58}. Likewise, autofluorescence imaging of cellular metabolism is useful for imaging immune cells as immune cell function is linked to cellular metabolism, and immune cell populations are often heterogeneous^{20,31}. Standard biochemical assays typically evaluate immune cells at the population level or require intracellular labeling following cell permeabilization^{34,59,60}. Autofluorescence imaging is also well-suited for high-resolution *in vivo* and dynamic measurements of metabolism due to the non-destructive nature of light and lack of chemical or genetically encoded labels^{36–38,41,48,55}. Critical steps for imaging NAD(P)H and FAD fluorescence intensity and lifetime include the selection of appropriate wavelengths for excitation and emission, verification that the cells do not contain synthetic or additional endogenous fluorophores that will contribute overlapping fluorescence, and the use of nondamaging laser powers.

Autofluorescence imaging of NAD(P)H and FAD fills a unique niche as a label-free, high-resolution, quantitative metabolic imaging technology. Other imaging methods, such as FDG-PET and MRS, image tissue metabolism but lack cellular level resolution and thus cannot evaluate cellular heterogeneity. Other biochemical techniques, such as oxygen consumption assays, measurements of metabolites in the media, or protein analysis, require expensive single-use reagents, obtain measurements from pooled cells, and require cell-destructive protocols, preventing time-course studies or *in vivo* analysis^{61,62}.

While autofluorescence imaging of NAD(P)H and FAD provides high-resolution images in a label-free and nondestructive manner, some limitations of autofluorescence imaging must be considered when designing and interpreting experiments. FLIM requires specialized and expensive equipment that is not widely available. The FLIM excitation requires a pulsed-excitation source with picosecond or femtosecond pulses at a repetition rate between 40 and 100 MHz with output power > 50 mW⁶³. Additionally, image acquisition is relatively slow, with a trade-off between the number of pixels or image resolution and image acquisition time. The parameters recommended in this protocol of 256 x 256 pixels and 60 s integration time provide an image with reasonable resolution within about 1 mi. The user can choose to image smaller areas with fewer pixels or perform line scans to improve the imaging speed.

Alternatively, higher-pixel images can be acquired with increased image integration times. The data analysis and interpretation of autofluorescence lifetime images can be challenging as FLIM

provides specific biophysical information about the metabolic coenzymes and their molecular environment rather than specific metabolic pathways. Optical microscopy is also limited by the depth of light penetration in tissue due to light scattering and absorption. *In vivo* studies can be done, at depths of ~0.5 mm with multiphoton imaging systems, of surface tissues or through window chambers^{2,20,21,64,65}.

While NAD(P)H and FAD are the primary endogenous fluorophores in isolated cells, additional molecules, including collagen and elastin, can contribute autofluorescence signals in tissues. The high-resolution images of multiphoton microscopy allow visualization of cellular and noncellular compartments for segmentation of NAD(P)H and FAD pixels from the extracellular proteins⁴⁰. Some cells contain endogenous molecules with overlapping fluorescence, such as lipofuscin, retinol, tryptophan, and melanin⁶⁶. Therefore, autofluorescence images of NAD(P)H and FAD may contain background contributions from other endogenous molecules.

Likewise, while NAD(P)H and FAD can be multiplexed with exogenous fluorophores that emit at wavelengths above 600 nm, exogenous labels, such as DAPI or genetically encoded proteins such as GFP, spectrally overlap with autofluorescence imaging. The cyanide perturbation experiment described here helps verify that the excitation and emission wavelengths isolate NAD(P)H and FAD sufficiently to capture metabolic changes in cells. Other cell types can be applied to this protocol; however, the user should optimize imaging parameters, including laser power and image integration time for each cell type, and experiment to prevent photobleaching. Photobleaching can be minimized by monitoring the photon count rate or average fluorescence intensity during imaging for the duration of the lifetime scan. An increase or decrease in fluorescence intensity indicates that the laser power is too high. If laser powers induce photobleaching, the power can be reduced, and the total image acquisition increased to achieve sufficient photon collection for lifetime analysis.

Although the fluorescence lifetimes are independent of imaging parameters, including laser power and detector gain, the fluorescence intensity is dependent on these parameters²⁰. Therefore, when conducting autofluorescence imaging to quantify the optical redox ratio, it is critical to use consistent imaging parameters. The protocol recommends that 5–6 images of different FOVs be acquired from each experimental group. This sample size provides sufficient data at both the image and cell levels to resolve the expected differences in fluorescence lifetime parameters of confluent MCF7 cells due to the cyanide perturbation. The optimal number of images acquired per group depends on the experimental design and effect size. When switching between NAD(P)H and FAD images, the focal plane should remain the same at each location for consistency. Although lifetime imaging typically does not have a saturating number of photons, intensity images acquired with cameras or photomultiplier tubes can be saturated. Pixel saturation should be avoided to ensure that the entire range of physiological intensities is captured in the images.

When analyzing fluorescence lifetime images, either a measured IRF or a simulated IRF can be used. The simulated IRF is estimated from the upshoot of the fluorescent lifetime curve; however, the real IRF obtained from the system might be broader depending on the system and thus result

in more accurate lifetime values. While the IRF typically only changes with hardware or software alterations, a daily IRF measurement is a good practice to ensure the fluorescence lifetime system is working as expected.

Overall, autofluorescence imaging of NAD(P)H and FAD provides a label-free, nondestructive method to image and analyze cellular metabolism at the single-cell level. This method provides a step-by-step approach to validate the imaging of NAD(P)H and FAD using cyanide to induce a well-characterized metabolic perturbation in cells.

ACKNOWLEDGMENTS:

Funding sources include the Cancer Prevention and Research Institute of Texas (CPRIT RP200668) and Texas A&M University. **Figure 1** was created with BioRender.com.

DISCLOSURES:

The authors have no conflicts of interest to disclose.

REFERENCES:

- 1 Heikal, A. A. Intracellular coenzymes as natural biomarkers for metabolic activities and mitochondrial anomalies. *Biomarkers in Medicine*. **4** (2), 241–263 (2010).
- 2 Georgakoudi, I., Quinn, K. P. Optical imaging using endogenous contrast to assess metabolic state. *Annual Review of Biomedical Engineering*. **14**, 351–367 (2012).
- 3 Zheng, J. Energy metabolism of cancer: Glycolysis versus oxidative phosphorylation (Review). *Oncology Letters*. **4** (6), 1151–1157 (2012).
- 4 Potter, M., Newport, E., Morten, K. J. The Warburg effect: 80 years on. *Biochemical Society Transactions*. **44** (5), 1499–1505 (2016).
- 5 Zhao, Y., Butler, E. B., Tan, M. Targeting cellular metabolism to improve cancer therapeutics. *Cell Death and Disease*. **4** (3), e532 (2013).
- 6 Patel, S., Ahmed, S. Emerging field of metabolomics: Big promise for cancer biomarker identification and drug discovery. *Journal of Pharmaceutical and Biomedical Analysis*. **107**, 63–74 (2015).
- 7 Walsh, A. J., Cook, R. S., Skala, M. C. Functional optical imaging of primary human tumor organoids: Development of a personalized drug screen. *Journal of Nuclear Medicine*. **58** (9), 1367–1372 (2017).
- 8 Zaal, E. A., Berkers, C. R. The influence of metabolism on drug response in cancer. *Frontiers in Oncology*. **8**, 500 (2018).
- 9 Little, A. C. et al. High-content fluorescence imaging with the metabolic flux assay reveals insights into mitochondrial properties and functions. *Communications Biology*. **3** (1), 271 (2020).
- 10 Wang, X. et al. Comparison of magnetic resonance spectroscopy and positron emission tomography in detection of tumor recurrence in posttreatment of glioma: A diagnostic meta-analysis. *Asia-Pacific Journal of Clinical Oncology*. **11** (2), 97–105 (2015).
- 11 Nabi, H. A., Zubeldia, J. M. Clinical applications of 18F-FDG in oncology. *Journal of Nuclear Medicine Technology*. **30** (1), 3–9 (2002).
- 12 Kostakoglu, L., Agress, H., Jr, Goldsmith, S. J. Clinical role of FDG PET in evaluation of cancer patients. *Radiographics*. **23** (2), 315–340 (2003).

791 13 Hoh, C. K. Clinical use of FDG PET. *Nuclear Medicine and Biology*. **34** (7), 737–742 (2007).
 792 14 van de Weijer, T., Schrauwen-Hinderling, V. B. Application of magnetic resonance
 793 spectroscopy in metabolic research. *Biochimica et Biophysica Acta. Molecular Basis of Disease*.
 794 **1865** (4), 741–748 (2019).
 795 15 Huang, S., Heikal, A. A., Webb, W. W. Two-photon fluorescence spectroscopy and
 796 microscopy of NAD(P)H and Flavoprotein. *Biophysical Journal*. **82**, 2811–2825 (2002).
 797 16 Lagarto, J. L. et al. Characterization of NAD(P)H and FAD autofluorescence signatures in a
 798 Langendorff isolated-perfused rat heart model. *Biomedical Optics Express*. **9** (10), 4961–4978
 799 (2018).
 800 17 Lakowicz, J. R. *Principles of fluorescence spectroscopy*. Springer, Boston, MA (2013).
 801 18 Lakowicz, J. R., Szmacinski, H., Nowaczyk, K., Johnson, M. L. Fluorescence lifetime imaging
 802 of free and protein-bound NADH. *Proceedings of the National Academy of the Sciences of the*
 803 *United States of America*. **89** (4), 1271–1275 (1992).
 804 19 Nakashima, N., Yoshihara, K., Tanaka, F., Yagi, K. Picosecond fluorescence lifetime of the
 805 coenzyme of D-amino acid oxidase. *Journal of Biological Chemistry*. **255** (11), 5261–5263 (1980).
 806 20 Hu, L., Wang, N., Cardona, E., Walsh, A. J. Fluorescence intensity and lifetime redox ratios
 807 detect metabolic perturbations in T cells. *Biomedical Optics Express*. **11** (10), 5674–5688 (2020).
 808 21 Datta, R., Heaster, T. M., Sharick, J. T., Gillette, A. A., Skala, M. C. Fluorescence lifetime
 809 imaging microscopy: fundamentals and advances in instrumentation, analysis, and applications.
 810 *Journal of Biomedical Optics*. **25** (7), 1–43 (2020).
 811 22 Liu, Z. et al. Mapping metabolic changes by noninvasive, multiparametric, high-resolution
 812 imaging using endogenous contrast. *Science Advances*. **4** (3), eaap9302 (2018).
 813 23 Georgakoudi, I., Quinn, K. P. Optical imaging using endogenous contrast to assess
 814 metabolic state. *Annual Review of Biomedical Engineering*. **14**, 351–367 (2012).
 815 24 Varone, A. et al. Endogenous two-photon fluorescence imaging elucidates metabolic
 816 changes related to enhanced glycolysis and glutamine consumption in precancerous epithelial
 817 tissues. *Cancer Research*. **74** (11), 3067–3075 (2014).
 818 25 Chance, B., Schoener, B., Oshino, R., Itshak, F., Nakase, Y. Oxidation-reduction ratio
 819 studies of mitochondria in freeze-trapped samples. NADH and flavoprotein fluorescence signals.
 820 *Journal of Biological Chemistry*. **254** (11), 4764–4771 (1979).
 821 26 Sharick, J. T. et al. Protein-bound NAD(P)H lifetime is sensitive to multiple fates of glucose
 822 carbon. *Scientific Reports*. **8** (1), 5456 (2018).
 823 27 Skala, M. C. et al. In vivo multiphoton microscopy of NADH and FAD redox states,
 824 fluorescence lifetimes, and cellular morphology in precancerous epithelia. *Proceedings of the*
 825 *National Academy of Sciences of the United States of America*. **104** (49), 19494–19499 (2007).
 826 28 Skala, M. C. et al. In vivo multiphoton fluorescence lifetime imaging of protein-bound and
 827 free nicotinamide adenine dinucleotide in normal and precancerous epithelia. *Journal of*
 828 *Biomedical Optics*. **12** (2), 024014 (2007).
 829 29 Uchugonova, A. A., König, K. Two-photon autofluorescence and second-harmonic imaging
 830 of adult stem cells. *Journal of Biomedical Optics*. **13** (5), 054068 (2008).
 831 30 Miranda-Lorenzo, I. et al. Intracellular autofluorescence: a biomarker for epithelial cancer
 832 stem cells. *Nature Methods*. **11** (11), 1161–1169 (2014).
 833 31 Walsh, A. J. et al. Classification of T-cell activation via autofluorescence lifetime imaging.
 834 *Nature Biomedical Engineering*. **5** (1), 77–88 (2021).

835 32 Heaster, T. M., Humayun, M., Yu, J., Beebe, D. J., Skala, M. C. Autofluorescence imaging
836 of 3D tumor-macrophage microscale cultures resolves spatial and temporal dynamics of
837 macrophage metabolism. *Cancer Research*. **80** (23), 5408–5423 (2020).

838 33 Pavillon, N., Hobro, A. J., Akira, S., Smith, N. I. Noninvasive detection of macrophage
839 activation with single-cell resolution through machine learning. *Proceedings of the National
840 Academy of Sciences of the United States of America*. **115** (12), E2676–E2685 (2018).

841 34 Chang, C. H. et al. Posttranscriptional control of T cell effector function by aerobic
842 glycolysis. *Cell*. **153** (6), 1239–1251 (2013).

843 35 Kaech, S. M., Cui, W. Transcriptional control of effector and memory CD8⁺ T cell
844 differentiation. *Nature Reviews. Immunology*. **12** (11), 749–761 (2012).

845 36 Gómez, C. A., Fu, B., Sakadžić, S., Yaseena, M. A. Cerebral metabolism in a mouse model
846 of Alzheimer’s disease characterized by two-photon fluorescence lifetime microscopy of intrinsic
847 NADH. *Neurophotonics*. **5** (4), 045008 (2018).

848 37 Yaseen, M. A. et al. In vivo imaging of cerebral energy metabolism with two-photon
849 fluorescence lifetime microscopy of NADH. *Biomedical Optics Express*. **4** (2), 307–321 (2013).

850 38 Bower, A. J. et al. High-speed label-free two-photon fluorescence microscopy of
851 metabolic transients during neuronal activity. *Applied Physics Letters*. **118** (8), 081104 (2021).

852 39 Walsh, A. J. et al. Quantitative optical imaging of primary tumor organoid metabolism
853 predicts drug response in breast cancer. *Cancer Research*. **74** (18), 5184–5194 (2014).

854 40 Walsh, A. J. et al. Optical metabolic imaging identifies glycolytic levels, subtypes, and
855 early-treatment response in breast cancer. *Cancer Research*. **73** (20), 6164–6174 (2013).

856 41 Chowdary, M. V. P. et al. Autofluorescence of breast tissues: Evaluation of discriminating
857 algorithms for diagnosis of normal, benign, and malignant conditions. *Photomedicine and Laser
858 Surgery*. **27** (2), 241–252 (2009).

859 42 Demos, S. G., Bold, R., White, R. D., Ramsamooj, R. Investigation of near-infrared
860 autofluorescence imaging for the detection of breast cancer. *IEEE Journal of Selected Topics in
861 Quantum Electronics*. **11** (4), 791–798 (2005).

862 43 Heaster, T. M., Humayun, M., Yu, J., Beebe, D. J., Skala, M. C. Autofluorescence imaging
863 of 3D tumor-macrophage microscale cultures resolves spatial and temporal dynamics of
864 macrophage metabolism. *Cancer Research*. **80** (23), 5408–5423 (2020).

865 44 Sharick, J. T. et al. Cellular metabolic heterogeneity in vivo is recapitulated in tumor
866 organoids. *Neoplasia*. **21** (6), 615–626 (2019).

867 45 Shah, A. T., Diggins, K. E., Walsh, A. J., Irish, J. M., Skala, M. C. In vivo autofluorescence
868 imaging of tumor heterogeneity in response to treatment. *Neoplasia*. **17** (12), 862–870 (2015).

869 46 Walsh, A. J., Skala, M. C. Optical metabolic imaging quantifies heterogeneous cell
870 populations. *Biomedical Optics Express*. **6** (2), 559–573 (2015).

871 47 Walsh, A. J., Skala, M. C. An automated image processing routine for segmentation of cell
872 cytoplasm in high-resolution autofluorescence images. *Multiphoton Microscopy in the
873 Biomedical Sciences XIV*. **89481M** (2014).

874 48 Skala, M., Ramanujam, N. *Methods in Molecular Biology*. **594**, 155–162 (2010).

875 49 Stringari, C. et al. Multicolor two-photon imaging of endogenous fluorophores in living
876 tissues by wavelength mixing. *Scientific Reports*. **7**, 3792 (2017).

877 50 SPCImage. SPCImage 2.9: Data analysis software for fluorescence lifetime imaging
878 microscopy. <https://biology.uiowa.edu/sites/biology.uiowa.edu/files/SPCIMAGE29.pdf> (2007)

- 51 CellProfiler. Download. <https://cellprofiler.org/releases> (2007).
- 52 GitHub. *Autofluorescence Imaging*. [https://github.com/walshlab/Autofluorescence-](https://github.com/walshlab/Autofluorescence-Imaging)
- 53 Ramey, N. A., Park, C. Y., Gehlbach, P. L., Chuck, R. S. Imaging mitochondria in living
corneal endothelial cells using autofluorescence microscopy. *Photochemistry and Photobiology*.
83 (6), 1325–1329 (2007).
- 54 Walsh, A., Cook, R. S., Rexer, B., Arteaga, C. L., Skala, M. C. Optical imaging of metabolism
in HER2 overexpressing breast cancer cells. *Biomedical Optics Express*. **3** (1), 75–85 (2012).
- 55 Kolenc, O. I., Quinn, K. P. Evaluating cell metabolism through autofluorescence imaging
of NAD(P)H and FAD. *Antioxidants & Redox Signaling*. **30**, 875–889 (2019).
- 56 Bird, D. K. et al. Metabolic mapping of MCF10A human breast cells via multiphoton
fluorescence lifetime imaging of the coenzyme NADH. *Cancer Research*. **65**, 8766–8773 (2005).
- 57 Walsh, A. J. et al. Optical metabolic imaging identifies glycolytic levels, subtypes, and
early-treatment response in breast cancer. *Cancer Research*. **73** (20), 6164–6174 (2013).
- 58 Walsh, A. J., Castellanos, J. A., Nagathihalli, N. S., Merchant, N. B., Skala, M. C. Optical
imaging of drug-induced metabolism changes in murine and human pancreatic cancer organoids
reveals heterogeneous drug response. *Pancreas*. **45** (6), 863–869 (2016).
- 59 Gubser, P. M. et al. Rapid effector function of memory CD8⁺ T cells requires an
immediate-early glycolytic switch. *Nature Immunology*. **14** (10), 1064–1072 (2013).
- 60 Papalexi, E., Satija, R. Single-cell RNA sequencing to explore immune cell heterogeneity.
Nature Review. Immunology. **18** (1), 35–45 (2018).
- 61 Horan, M. P., Pichaud, N., Ballard, J. W. O. Review: Quantifying mitochondrial dysfunction
in complex diseases of aging. *The Journals of Gerontology: Series A*. **67** (10), 1022–1035 (2012).
- 62 Plitzko, B., Loesgen, S. Measurement of oxygen consumption rate (OCR) and extracellular
acidification rate (ECAR) in culture cells for assessment of the energy metabolism. *Bio-protocol*.
8 (10), e2850 (2018).
- 63 Becker, W. The bh TCSPC Handbook. [https://www.becker-hickl.com/wp-](https://www.becker-hickl.com/wp-content/uploads/2021/10/SPC-handbook-9ed-05a.pdf)
- 64 Gadella, T. W. J. in *Fluorescent and Luminescent Probes for Biological Activity*.
<https://doi.org/10.1016/B978-012447836-7/50036-1> Mason, W. T. (Ed) Ch. 34, 467–479 (1999).
- 65 Miller, D. R., Jarrett, J. W., Hassan, A. M., Dunna, A. K. Deep tissue imaging with
multiphoton fluorescence microscopy. *Current Opinion in Biomedical Engineering*. **4**, 32–39
(2017).
- 66 Berezin, M. Y., Achilefu, S. Fluorescence lifetime measurements and biological imaging.
Chemical Reviews. **110** (5), 2641–2684 (2010).

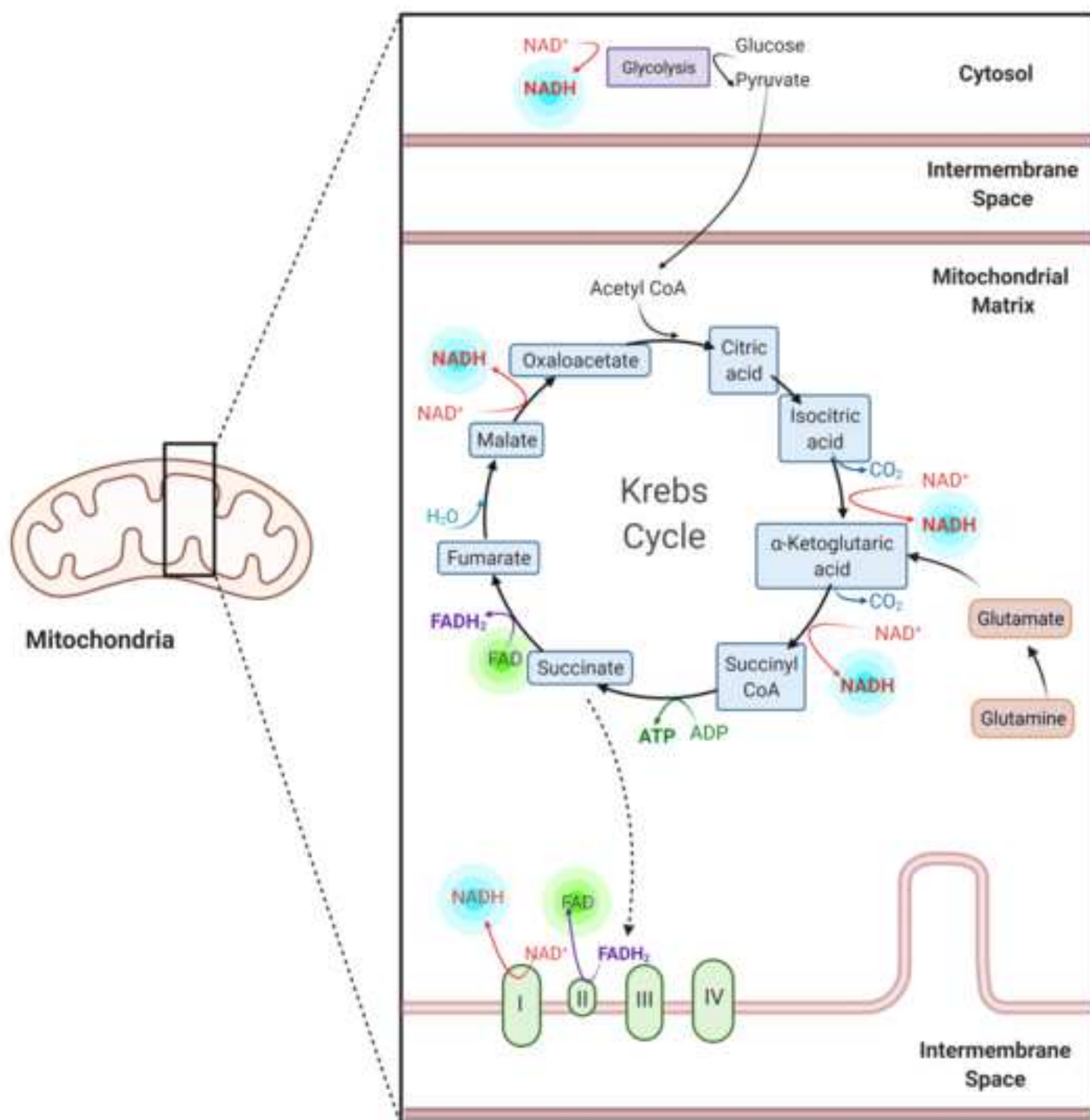
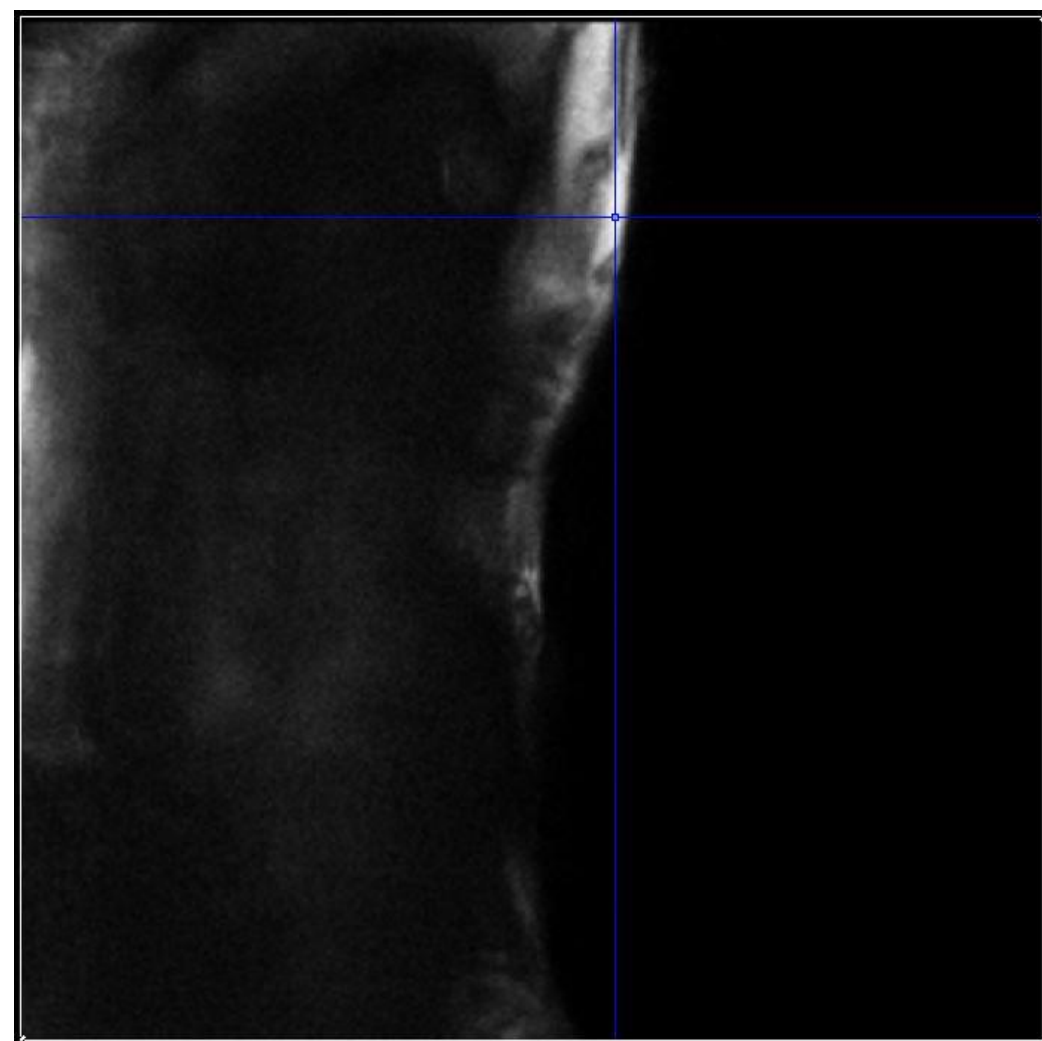
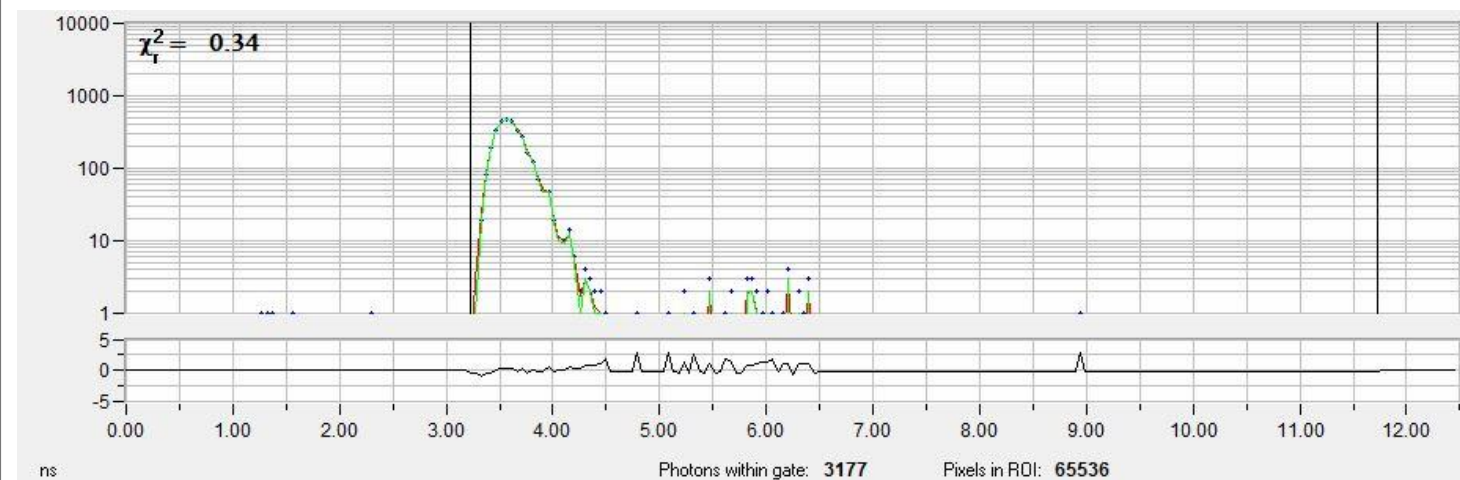


Figure 2

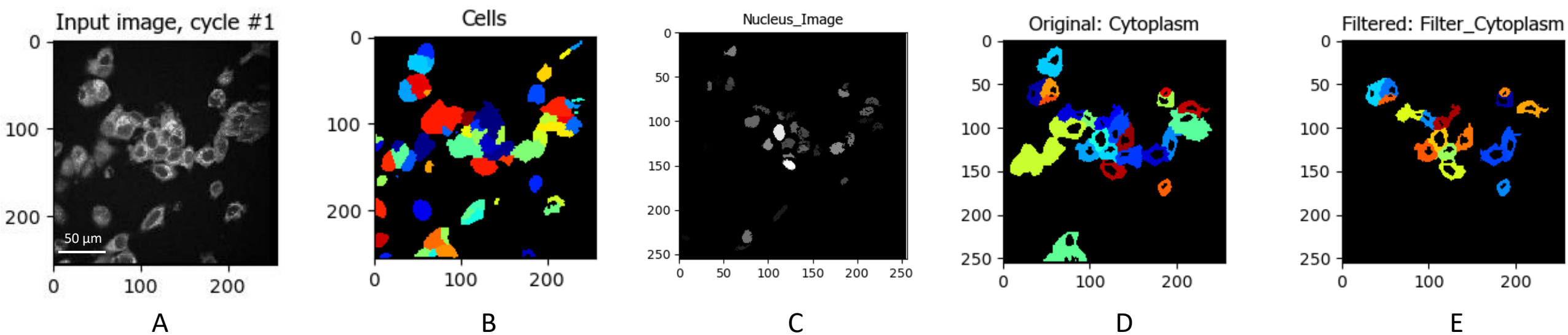
[Click here to access/download;Figure;Figure 2.pdf](#)



A



B



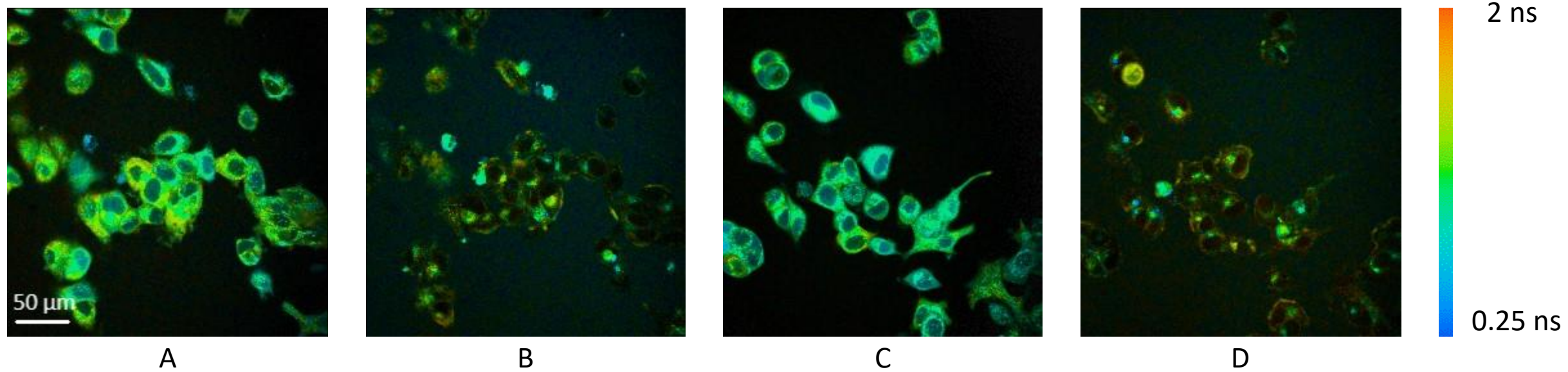


Figure 5

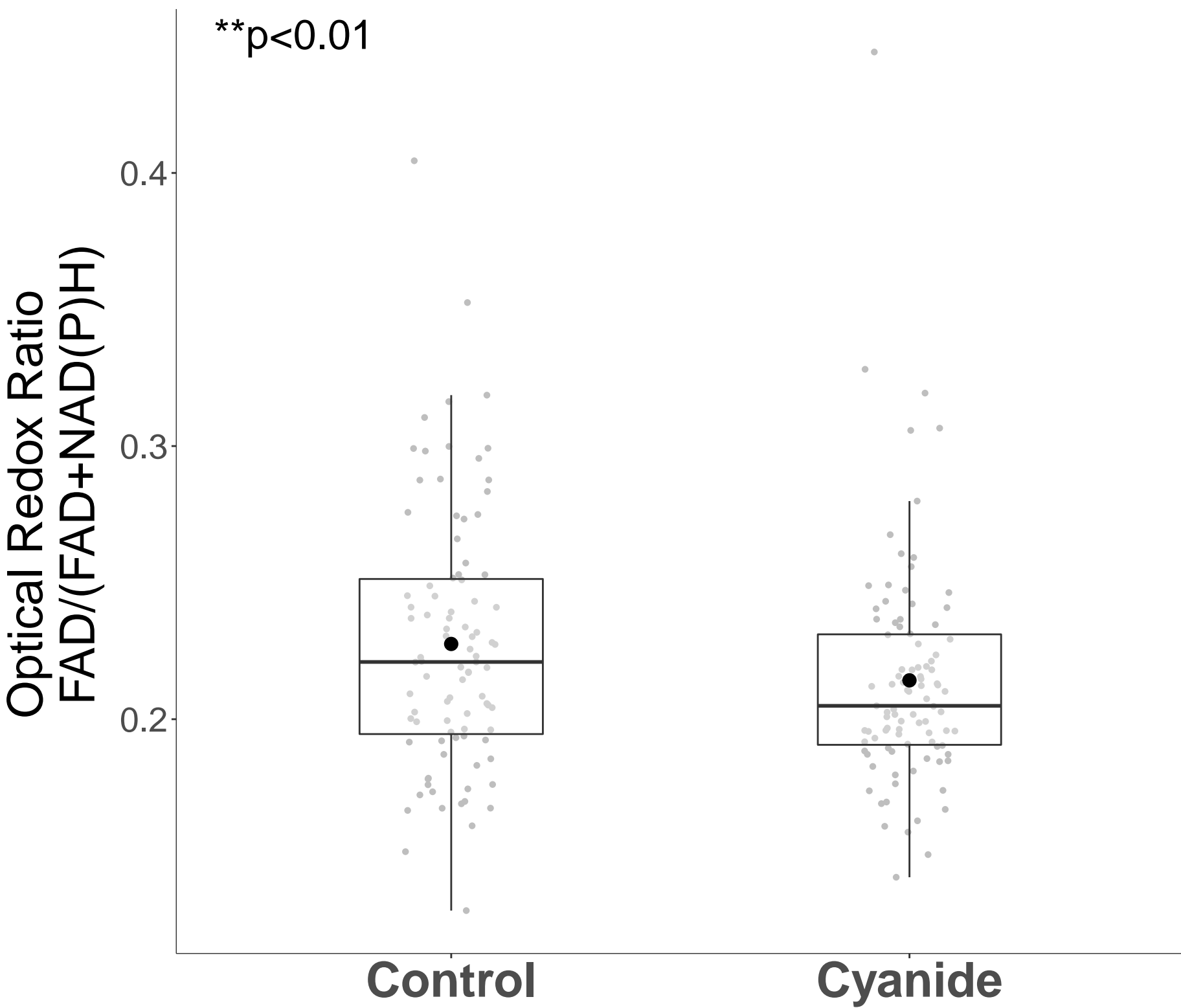


Figure 6

[Click here to access/download;Figure;Figure 6.pdf](#)

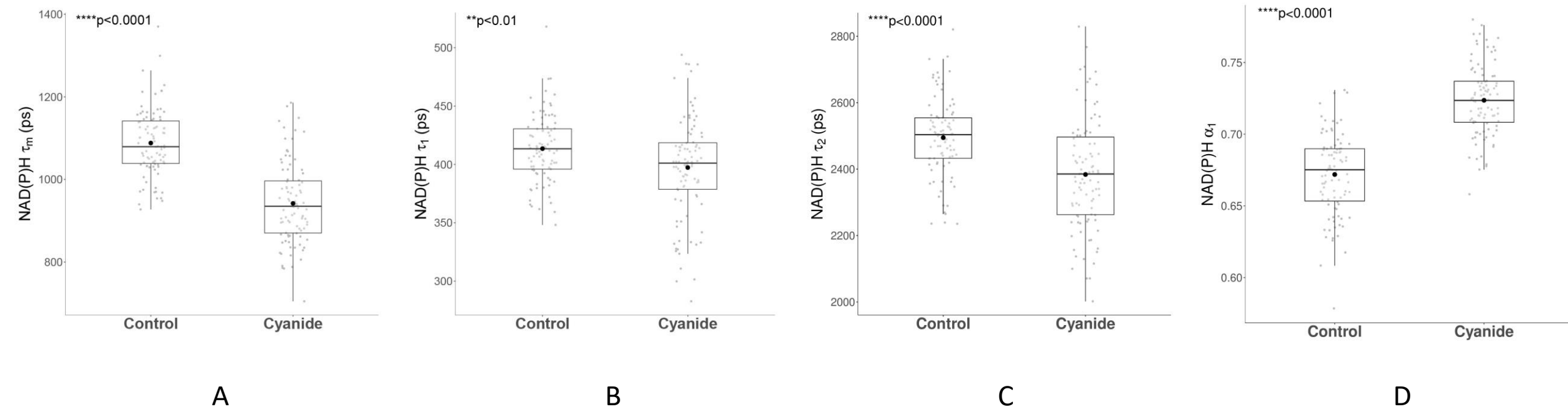
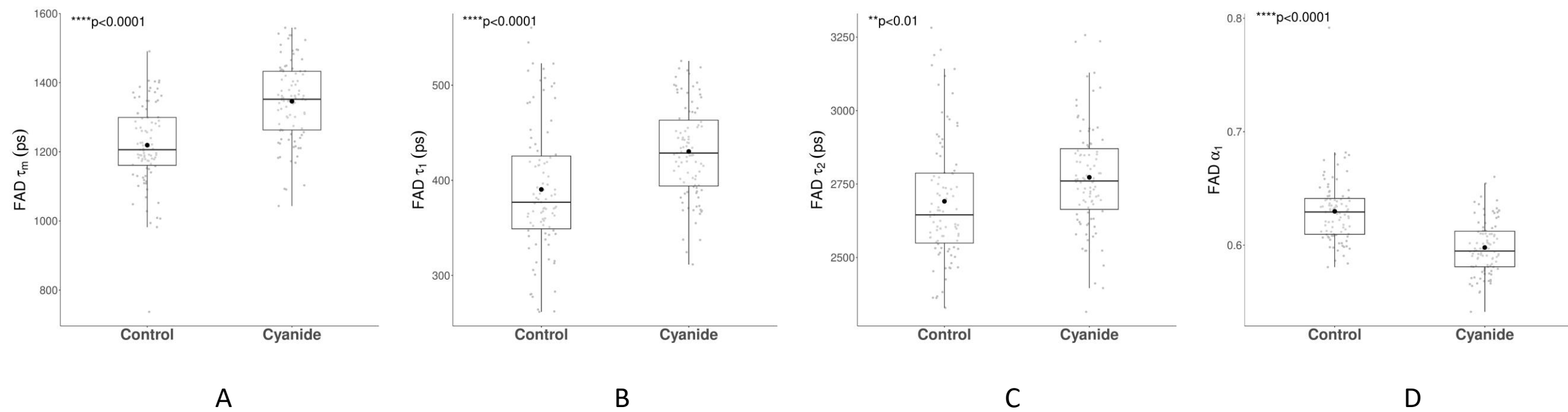


Figure 7

[Click here to access/download;Figure;Figure 7.pdf](#)





[Click here to access/download](#)

Table of Materials
JoVE_Table_of_Materials (6).xlsx



Editorial comments:

Editorial Changes

Changes to be made by the Author(s):

1. Please take this opportunity to thoroughly proofread the manuscript to ensure that there are no spelling or grammar issues.

We have proofread the manuscript for spelling and grammar.

2. For in-text formatting, corresponding reference numbers should appear as numbered superscripts after the appropriate statement(s) before the punctuation.

We have changed the in-text citations to numbered superscripts before the punctuation.

3. JoVE cannot publish manuscripts containing commercial language. This includes trademark symbols (™), registered symbols (®), and company names before an instrument or reagent. Please remove all commercial language from your manuscript and use generic terms instead. All commercial products should be sufficiently referenced in the Table of Materials. For example Agilent’s Seahorse Assays, YG bead, Polysciences Inc, 3i system, SPCImage, etc.

We understand to follow the JoVE guidelines. We made revisions to exclude any commercial product names in the manuscript. This includes any mention of software names, such as CellProfiler and SPCImage in the protocol. We have added citations so the user can find the software used in the protocol for their own experiments.

4. The Protocol should contain only action items that direct the reader to do something. Any text that provides details about how to perform a particular step should either be included in the step itself or added as a sub-step. Please move additional protocol information to either the discussion or introduction.

We have reviewed the protocol and put any additional protocol information within the discussion.

For example, the commentary, “All living cells will exhibit endogenous NAD(P)H and FAD fluorescence ...” is repetitive with the introduction and has been removed from Step 1 of the Protocol.

5. Please define all abbreviations before use. For example, GFP, DAPI, YG, etc.

We have added the definitions to all abbreviations when first mentioned in the manuscript. See line 483, 489, and 204.

6. Please adjust the numbering of the Protocol to follow the JoVE Instructions for Authors. For example, 1 should be followed by 1.1 and then 1.1.1 and 1.1.2 if necessary. For example, 1. Cell plating for imaging followed by 1.1 Starting with a confluent... and so on.

The Protocol numbering has been updated to match the JoVE Instructions.

7. Please revise the text to avoid the use of any personal pronouns (e.g., "we", "you", "our" etc.). Please avoid the usage of phrases such as "could be," "should be," and "would be" throughout the Protocol.

We have removed all personal pronouns and "could be", "should be" and "would be" throughout the Protocol.

8. Please add more details to your protocol steps. Please ensure you answer the "how" question, i.e., how is the step performed?

We understand that this will make the protocol easier for the reader to follow. We have included more of where the user should click in the software as suggested. For these parts we specified, we have also noted in parenthesis that this specific to the image acquisition software and image analysis software of our system but may be modified for systems by different manufacturers. For example, see Step 2.2.4 and 4.2.4 were changed to be more specific for the user.

Line 133: At what confluency were the cells used for experimentation?

The cells were at 80-90% confluency. We have made this addition, Protocol 1.1:

"1.1. Aspirate the media from an 80-90% confluent T-75 flask of MCF-7 cells, rinse the cells with 10 mL sterile PBS (Phosphate-buffered saline) and add 2 mL 0.25% trypsin (1X) to detach the cells from the flask bottom. "

Line 145: Please provide centrifugal force calculated in x g for centrifugation.

We centrifuged the cells at 200 xg. We have made the following revision below, Protocol 1.5:

"Centrifuge the cells 200 xg for 5 minutes."

Line 151: The cells were grown at 37 °C? If yes, please specify. Please provide incubation conditions. How was the logarithmic growth phase identified?

The cells were grown at 37 °C. We made sure to specify this in the protocol. Additionally, the logarithmic growth phase was identified by the cell's data sheet on the company's website.

"Incubate the cells at 37 °C with 5% CO₂ for 24-48 hr prior to imaging for cells to adhere and reach the logarithmic growth phase (the growth phase was determined by prior experience with these cells and confirmed with the cell data sheet). "

Line 161,178: Please include button clicks in the software, command lines, etc. for starting the microscope and setting up the image acquisition software.

We understand that this will make the protocol easier for the reader to follow. We have added software clicks and noted that these are specific to the Slidebook image acquisition software and may be adapted to different microscopes. Here are the following revisions we have made based off the comment:

“Turn on all components of the multiphoton fluorescence lifetime microscope including the microscope, the laser source, and the detectors being used. “

“If the microscope is within an enclosure, close the lightbox door. Open the image acquisition software, click on the **Multiphoton Imaging** tab and set desired multiphoton imaging parameters.”

Line 204: What are the recommended image parameters? Please specify. Alternatively, add references to published material for the parameters.

We thank the reviewer for bringing us to our attention. We have directed the readers to step 2.2.4, which has the recommended imaging parameters for multiphoton imaging. These are identical for our recommended parameters for the IRF image acquisition. Here is the revision below:

“Obtain a fluorescence lifetime image of the YG bead using a laser power at the sample <1 mW and recommended image parameters [Step 2.2.4].”

Line 327: What was the final bin value?

The final bin value for our experiment was one. We did not require additional binning in our images. This might be dependent on the user however, so we made the following revision below:

“Import urea image. Select a point on the image of the urea crystal to be used for image analysis. Increase the spatial bin value to integrate FLIM data from multiple pixels to 1 or higher for a decay peak > 100 photons.”

Line 343: what were the parameter values used in the protocol? How were they set?

We have added what the user should optimize when setting the parameters. We have also included a reference for the SPCImage manual for the reader.

- Set a threshold value to evaluate decays for cytoplasm pixels. Here, a value of 50 was used. The value was selected by comparing the fluorescence peak values of several representative background and nucleus pixels with the peak value of several cytoplasm pixels. A value between the nucleus pixels and cytoplasm pixels was selected for the threshold.
- Check that the Shift value aligns the IRF relative to the rising edge of the fluorescence. Adjust the shift if needed to a value that minimizes the Chi-squared value.
- Increase spatial bin so cytoplasm pixels have fluorescence peak values at or above 100. Note that increasing the spatial bin, will lead to decreased spatial resolution.

Line 372: Please provide all website links in the references. The reference can then be cited in the text.

We have made an endnote custom entry reference with the corresponding links attached.

Line 377: Is it 0-1? Please check.

Yes. The CellProfiler module “Rescale intensity” normalizes the pixel values from 0 (blackest pixel color) to 1 (whitest pixel color). “

9. Please include all the Figure Legends together at the end of the Representative Results in the manuscript text.

All Figure Legends have been added at the end of the Representative Results section.

10. Figure 3: what do the x-axis and y-axis represent?

We thank the reviewer for bringing this to our attention. We have included what the x-axis and y-axis represent in the figure caption, as seen below:

“Figure 3: Identification and segmentation of individual cells. The NAD(P)H intensity image of MCF7 cells obtained by integrating a fluorescence lifetime image. Cells were imaged using 750 nm excitation at 5 mW for 60 seconds. The x and y axis represent the pixel location of the image. **(A)** was used to identify individual cells. The cells were masked **(B)** in order to eliminate any background noise from the data set. The nucleus was then identified **(C)** and projected onto the cell mask **(D)**. The cells were then filtered **(E)** to remove masked areas that do not fit the size of typical cells. “

11. Figure 4: what does the color bar represent?

The Figure 4 caption has been amended to include, “The amplitude-weighted fluorescence lifetime (indicated by the color bar) measures the time a fluorophore, in these cases NAD(P)H and FAD, is in an excited state.”

12. Please also include the critical steps within the protocol in the Discussion.

Several critical considerations have been added to the Discussion to address several of the reviewer comments including a discussion of laser parameters, number of images to acquire, the trade off between laser power, image resolution, and image acquisition time. Additionally, we have included the following:

Critical steps for imaging NAD(P)H and FAD fluorescence intensity and lifetime include the selection of appropriate wavelengths for excitation and emission, verification that the cells do not contain synthetic or additional endogenous fluorophores that will contribute overlapping fluorescence, and the use of non-damaging laser powers.

13. Please ensure that the references appear as the following: [LastName, F.I., LastName, F.I., LastName, F.I. Article Title. Source. Volume (Issue), FirstPage – LastPage (YEAR).] For more than 6 authors, list only the first author then et al.

We have checked for the following and ensured that the references appeared in the same format.

14. Please include the catalog number of all relevant materials in the table of materials.

We have included catalog numbers for all materials in the table of materials. For items without a catalog number, are marked with NA (not applicable).

15. With regards to video production, please let us know how you would like to proceed. Please select one of the options below.

1. Journal Produced Videos (JPV): If you are within our videographer network, you can choose the Video Produced by JoVE option (<https://www.jove.com/authors/faq>). Once the manuscript is accepted, we write the script, film the protocol, and produce the video for you. If selecting this option please provide us with the complete filming address.

Filming address:
ETB 1040
Emerging Technologies Bldg Room 1040
3120 TAMU
101 Bizzell St
College Station, TX 77843-3120

2. Hybrid filming option (APF). In this case, upon manuscript acceptance, we write the script for you, you will then perform the filming and send us the raw footage straight out of the camera. Using these video clips, we will then produce the video for you. Please see the attached criteria. You do not need to film till the scripting is done.

Reviewers' comments:

Reviewer #1:

Manuscript Summary:

Theodossiou et al. describe a protocol for fluorescence lifetime imaging microscopy (FLIM) of endogenous metabolic co-enzymes NAD(P)H and FAD for label-free imaging of cellular metabolism. They focus this protocol on multiphoton FLIM, but also offer parallel settings for one-photon imaging. They also center the protocol on time-resolved imaging for a more complete metabolic imaging approach but provide an alternative protocol for intensity-based only fluorescence imaging to measure optical redox ratio. The protocol includes cell work and experimental preparation, instrument setup, imaging steps, and image analysis. The proposed experiment using cyanide serves as a validation method for NAD(P)H and FAD detection. The protocol is well explained, appears reproducible, it is mindful of alternative

setups, and it is relevant to the fluorescence lifetime imaging community. My recommendation is publish after minor revision.

Major Concerns:

The definition of mean lifetime as $\tau_m = \alpha_1\tau_1 + \alpha_2\tau_2$ is technically an amplitude-weighted lifetime. The average lifetime, or average amount of time a fluorophore is in the excited state, is computed by averaging "t" over the intensity decay of the fluorophore, which for a two-exponential decay results in $\tau_m = (\alpha_1\tau_1^2 + \alpha_2\tau_2^2)/(\alpha_1\tau_1 + \alpha_2\tau_2)$ (see ref 16 of this protocol). Being explicit about the distinction will help avoid confusion, especially for new incorporations into the field, for whom this protocol will be specially useful.

We appreciate the reviewer's key to detail. We have addressed this comment by clarifying that the τ_m used here is the amplitude-weighted lifetime.

"The amplitude-weighted lifetime, represented here as τ_m , is calculated as $\tau_m = \alpha_1\tau_1 + \alpha_2\tau_2$. A mean lifetime can be computed by averaging "t" over the intensity decay of the fluorophore, which for a two-exponential decay is $\tau_m^* = (\alpha_1\tau_1^2 + \alpha_2\tau_2^2)/(\alpha_1\tau_1 + \alpha_2\tau_2)$ ^{17,21}."

Minor Concerns:

Please revise for consistency with naming (for example, co-enzymes vs coenzymes) and grammar.

We have revised the manuscript for consistency and grammar.

Reviewer #2:

Manuscript Summary:

In this article the author describes how one can benefit in measuring cellular metabolism using FLIM and intensity-based approach. The author provided appropriate protocols for both methods as an example in measuring the metabolic perturbation by cyanide in MCF-7 cell lines. The results are clear demonstration of these techniques. The reader could follow this protocol if anyone would like to implement these approaches to monitor the metabolic changes in living cells.

Minor Concerns:

1. The author expect any photobleaching for 5-10 mW average power at the specimen plane for 60s data collection?

If the power is too high, photobleaching will occur at the sample. We have verified that our scanning parameters do not induce photobleaching. This was done by monitoring the photon count rate during image collection and plotting the intensity changes as a function of time. There was no change in intensity of the cells within 1.5 minutes of imaging at this power. We included this in the discussion. Here is the revision below:

"Other cell types can be applied to this protocol; however, the user should optimize imaging parameters including laser power and image integration time for each cell type and experiment to prevent photobleaching. Photobleaching can be minimized by monitoring the photon count rate or average fluorescence intensity during imaging for the duration of the lifetime scan. An increase or decrease in

fluorescence intensity indicates the laser power is too high. If laser powers induce photobleaching, the power can be reduced and the total image acquisition increased to achieve sufficient photon collection for lifetime analysis. “

2. How many photons per pixel is required for appropriate fitting of the FLIM data?

We thank the reviewer for bringing this up. There should be at least 100 photons per cytoplasm pixel for appropriate fitting of the FLIM data. Data can be spatially binned in SPCImage, if needed to increase the number of photons within the decay curve; however, spatial binning will decrease the spatial resolution. We have added this as a note in the image acquisition section of the protocol. Here is the revision below:

- Set a threshold value to evaluate decays for cytoplasm pixels. Here, a value of 50 was used. The value was selected by comparing the fluorescence peak values of several representative background and nucleus pixels with the peak value of several cytoplasm pixels. A value between the nucleus pixels and cytoplasm pixels was selected for the threshold.
- Check that the Shift value aligns the IRF relative to the rising edge of the fluorescence. Adjust the shift if needed to a value that minimizes the Chi-squared value.
- Increase spatial bin so cytoplasm pixels have fluorescence peak values at or above 100. Note that increasing the spatial bin, will lead to decreased spatial resolution.

3. The author should mention the FLIM company name. I believe the data was collected using Becker & Hickl, Germany.

We have to refrain from including the company name within the paper in order to follow JoVE guidelines. The companies and product numbers are included in the materials table.

4. Is it necessary to collect the instrument response function (IRF)? what will be the difference if the user uses the simulated IRF in the SPCImage data analysis software? It will be good to comment about the usage of the IRF for the data analysis.

We appreciate this thoughtful comment. The IRF is not necessary to collect; however, it is recommended that the user analyze the data with a measured IRF since in reality, the IRF is typically broader than the simulated IRF. This error is more pronounced for short lifetimes such as FAD τ_1 .

“When analyzing fluorescence lifetime images, either a measured IRF or a simulated IRF can be used. The simulated IRF is estimated from the upshoot of the fluorescent lifetime curve; however, the real IRF obtained from the system might be broader depending on the system and thus result in more accurate lifetime values. While the IRF typically only changes with hardware or software alterations, a daily IRF measurement is a good practice to ensure the fluorescence lifetime system is working as expected.”

5. The author should mention exactly what average power used at the specimen plane and the time for data collection in Figures 3 & 4 caption.

We appreciate this suggestion. We have included the power and time for data collection in both of the figures. Here is the revision of both captions from Figure 3 and Figure 4.

“Figure 3: Identification and segmentation of individual cells. The NAD(P)H intensity image of MCF7 cells (A) obtained by integrating a fluorescence lifetime image. Cells were imaged using 750 nm excitation at 5 mW for 60 seconds. The x and y axis represent the pixel location of the image. (A) was used to identify individual cells. The cells were masked (B) in order to eliminate any background noise from the data set. The nucleus was then identified (C) and projected onto the cell mask (D). The cells were then filtered (E) to remove masked areas that do not fit the size of typical cells. “

“Figure 4: Representative fluorescence lifetime images of MCF7 cells before and after cyanide treatment. (A) NAD(P)H amplitude-weighted fluorescence lifetime image and (B) FAD amplitude-weighted fluorescence lifetime image before cyanide treatment. (C) NAD(P)H amplitude-weighted fluorescence lifetime image and (D) FAD amplitude-weighted fluorescence lifetime image after cyanide treatment. The amplitude-weighted fluorescence lifetime (indicated by the color bar) measures the time a fluorophore, in these cases NAD(P)H and FAD, is in an excited state. NAD(P)H lifetime decreases with cyanide treatment, whereas the FAD lifetime increases after cyanide treatment. NADH signal was imaged using 750 nm excitation at 5 mW for 60 seconds and the FAD signal was imaged using 890 nm excitation at 7 mW for 60 seconds. Images acquired with a 40X water-immersion objective, NA=1.1. “

Reviewer #3:

Manuscript Summary:

The JoVE attempts to standardize a protocol for FLIM imaging of autofluorescence in order to guide the research field in metabolic mapping and profiling of cells. Both NAD(P)H and FAD autofluorescence detection procedures were demonstrated with excited state lifetime calculations to demonstrate shifts owing to the bound and unbound state of each respective metabolite. The use of cyanide to elicit a metabolic profile (e.g. glycolysis) was standardized. There was ample discussion of lifetime contributions including how alpha 1 parameter contributes to the proportional component of short vs long lifetimes i

Major Concerns:

None

Minor Concerns:

Will the calibration fluorophores used be reliable in terms of an absolute lifetime value as part of the two-step process?

We thank the reviewer for bringing up this question. The YG Bead fluorescence lifetime is stable over time provided that the beads remain in solution. We have included this in the protocol:

“Check the lifetime of the bead, using the IRF of the urea. The lifetime is stable over time and has a lifetime of ~2.1 ns.”

The protocol instructions could be somewhat hard to follow for those not familiar with cell segmentation. However the figures were well done and explained clearly.

We agree that the segmentation protocol might be hard to use for someone not familiar with CellProfiler. We have added more details to the protocol to allow the user to understand what the program does at each step.

Additional explanation would be helpful in figure 4, which seems to show both short and long lifetimes of NAD(P)H both decreasing with cyanide treatment. Meaning elaboration on the "contributions" of the both short and long lifetimes increase (or decrease with FAD) for NAD(P)H with cyanide treatment would be helpful.

We thank the reviewer for this helpful comment. We agree that we should add what changes are seen as a result of the cyanide treatment. Figure 4 is a visual representation of how the overall lifetime changes as a result of cyanide treatment in both NAD(P)H and FAD. The NAD(P)H lifetime decreases as a result of cyanide treatment and the FAD lifetime increases as a result of the lifetime. This can also be seen in subsequent figures, particularly in Figure 6 and Figure 7. Here is the revision we made:

“Figure 4: Representative fluorescence lifetime images of MCF7 cells before and after cyanide treatment. (A) NAD(P)H amplitude-weighted fluorescence lifetime image and (B) FAD amplitude-weighted fluorescence lifetime image before cyanide treatment. (C) NAD(P)H amplitude-weighted fluorescence lifetime image and (D) FAD amplitude-weighted fluorescence lifetime image after cyanide treatment. The amplitude-weighted fluorescence lifetime (indicated by the color bar) measures the time a fluorophore, in these cases NAD(P)H and FAD, is in an excited state. NAD(P)H lifetime decreases with cyanide treatment, whereas the FAD lifetime increases after cyanide treatment. NADH signal was imaged using 750 nm excitation at 5 mW for 60 seconds and the FAD signal was imaged using 890 nm excitation at 7 mW for 60 seconds. Images acquired with a 40X water-immersion objective, NA=1.1.”

Reviewer #4:

This manuscript by the Walsh group provides a nice overview of NAD(P)H and FAD autofluorescence imaging with an emphasis on FLIM techniques. Overall, this is a good overall review of the method, and there are some minor issues that should be addressed:

1) Line 36, the authors indicate healthy cells generate energy through oxidative phosphorylation in contrast to cancer cells that rely on glycolysis. This oversimplifies the differences among cell types and phenotypes in healthy cells. Many healthy but proliferative cells will rely heavily on glycolysis too.

Thank you for this comment. We agree that our statement was an oversimplification of the metabolic pathways healthy cells generate energy from. We have removed the statement that healthy cells rely on oxidative phosphorylation:

“Metabolism is the cellular process of producing energy. Cellular metabolism encompasses multiple pathways including glycolysis, oxidative phosphorylation, and glutaminolysis. Healthy cells use these metabolic pathways to generate energy for proliferation and function, such as the production of cytokines by immune cells. Many diseases, including metabolic disorders, cancer, and neurodegeneration, are characterized by altered cellular metabolism¹. For example, some cancer cell

types have elevated rates of glycolysis, even in the presence of oxygen, to generate molecules for the synthesis of nucleic acids, proteins, and lipids^{2,3}”

2) Line 48, it might help to clarify that Seahorse analyzers measure oxygen consumption rates.

We thank the reviewer for this clarification. We had to generalize this statement by omitting the Seahorse analyzer name to follow JoVE publishing guidelines. Here is the revision:

“Metabolic plate reader based assays can measure pH and oxygen consumption in the sample over time and following metabolic perturbation by chemicals”

3) Line 72, I believe the authors mean NADPH not NAD(P)H at the beginning of the sentence. As written, the sentence is very confusing.

We thank you for giving this distinction. We have reworded the sentence to help the readers better understand what we are trying to communicate.

“NADPH has similar fluorescent properties to NADH. Because of this, NAD(P)H is often used to represent the combined signal of both NADH and NADPH ^{2,16}.”

4) Line 88, the authors may want to use autofluorescence rather than autofluorescent.

We agree with the reviewer and thank them for this change. We have made the following change below.

“Autofluorescence imaging is a non-destructive and label-free method that can be used to characterize the metabolism of live cells at a subcellular resolution “

5) Line 89, the authors should define the optical redox ratio here when the term is first used.

We agree that the optical redox ratio should be more clearly defined when first mentioned. We have added an additional sentence that further explains the meaning.

“The optical redox ratio provides an optical analog metric of the chemical redox state of the cell and is calculated as the ratio of NAD(P)H and FAD intensities. Although the formula for calculating the optical redox ratio is not standardized²²⁻²⁵, here it is defined as the intensity of FAD over the combined intensities of NAD(P)H and FAD. This definition is used because the summed intensity in the denominator normalizes the metric between 0 and 1 and the expected result of the cyanide inhibition is a decrease in redox ratio.”

6) Lines 108-111, the authors should more clearly define peak excitation and emission and differentiate it from the broader range of reasonable wavelengths that can be used for NAD(P)H and FAD imaging. For example, NAD(P)H will excite below 740nm, and FAD will excite well below 890nm. This is important for readers to understand. The emission ranges are more clearly defined but the FAD wavelengths seem a bit red shifted.

We agree that NAD(P)H and FAD can be excited at a broader range of wavelengths and have made the following revision:

“In two photon fluorescence excitation, NAD(P)H and FAD will excite at wavelengths of approximately 700 to 750 nm and 700 to 900 nm respectively ^{15,49}.”

7) Line 157, the excitation wavelengths stated are not required. However, they may be recommended or optimal. This should be revised.

We agree with the reviewer’s suggestion. Although not required, the wavelengths used are recommended. We have made the edit for the user using the revision below:

“Note: 750 nm excitation is recommended for NAD(P)H although it has broad absorption 700-750 nm.”

“Note: 890 nm excitation is recommended for FAD although it has broad absorption 700-900 nm.”

8) Lines 181-185, it is not clear why these parameters are listed. Why should the image size be 256x256 pixels? This seems arbitrary, and excessively coarse. Should the integration time always be 60s? Many groups use different times. Some more information on optimal detector gain should be provided too. What is optimal for photon counting may not be optimal for intensity measurements in the alternative method.

We appreciate this thoughtful comment and agree that there should be an explanation provided as to why these parameters are recommended. We use these parameters for our experiments in order to maximize image resolution while still obtaining them within a reasonable time. With larger image sizes, it will take longer to acquire the image since there are more pixels (for example, a 1024x1024 pixel images has 16x as many pixels and would require 16x the imaging time). Although recommended, these parameters are not required for the reader to use. We have clearly marked the parameters as recommended in the protocol and explained the trade-off between resolution and image size within the discussion.

“Additionally, image acquisition is relatively slow with a trade-off between the number of pixels or image resolution and image acquisition time. The parameters recommended in this protocol of 256x256 pixels, 60 s integration time provide an image with reasonable resolution within about 1 minute. The user can choose to image smaller areas with fewer pixels or perform line scans to improve the imaging speed. Alternatively, higher pixel images can be acquired with increased image integration times”

Yes, the optimal detector gain for photon counting may not be the same as what is optimal for intensity measurements. We included that the optimal detector gain might vary depending on the manufacturer. We have added this as a note to make it more clear to the reader. Here is the revision below:

“Note: There is an optimized detector gain for operating detectors in single-photon counting mode, for the system referenced the value is 85%. “

9) Some requirements for the laser source should be provided. What is the recommended power? Are

there limitations for the acceptable pulse width and repetition rate? Is there a minimum time that one should wait between tuning the laser from 750nm to 890nm?

We have revised the manuscript (Discussion, page 16) to include requirements for the laser source. Since low powers are needed for imaging (<10 mW at the sample), the laser output power is typically not a limiting factor.

“The FLIM excitation requires a pulsed-excitation source with picosecond or femtosecond pulses at a repetition rate between 40 to 100 MHz with output power >50mW⁶¹.”

It is important to wait till laser is mode-locked after tuning to a new wavelength before imaging; however, the time for this to happen is typically very quick. We added this into the protocol. Here is the revision:

“Set the multiphoton laser to 890 nm and wait for it to mode-lock at the new wavelength. “

10) Does the IRF change daily, requiring urea measurements every time?

We thank you for commenting on this issue. In the lab, it is best practice to measure the IRF everyday. By doing so, we can ensure that the system is not changing in anyway and it operating correctly for measuring lifetime events. However, in reality the system should not change unless there are hardware or software alterations.

“When analyzing fluorescence lifetime images, either a measured IRF or a simulated IRF can be used. The simulated IRF is estimated from the upshoot of the fluorescent lifetime curve; however, the real IRF obtained from the system might be broader depending on the system and thus result in more accurate lifetime values. While the IRF typically only changes with hardware or software alterations, a daily IRF measurement is a good practice to ensure the fluorescence lifetime system is working as expected. “

11) A section on troubleshooting might be helpful. What if the bead lifetime is not 2.1 ns?

We agree that a troubleshooting section might be helpful to include throughout the protocol section. If the bead lifetime is not 2.1 ns, the following problems could have occurred:

- If beads are close to one another, quenching could occur and lower the lifetime
- If solution dries out, the lifetime can be different
- If beads are not in focus, scattered light might be appearing in the image
- A poor lifetime fit due to an unrepresentative IRF or IRF shift

We have added this revision for the user:

“Check the lifetime of the bead, using the IRF of the urea. The lifetime is stable over time and has a lifetime of ~2.1 ns.

Note: If the lifetime is not ~2.1 ns, check the following:

- Bead is in contact with another bead contributing to fluorescence quenching
- Bead solution has dried

- Bead is out of focus
- IRF is not accurate or shift between IRF and fluorescence decay is not optimized [see **Step 4.2.4.**]

12) Line 231, is live cell metabolism sensitive to temperature and CO₂ levels? Should a chamber be recommended?

This is a great point to include! The metabolism of live cells is sensitive to temperature and CO₂ levels. An environmental chamber is recommended to the user because the chamber can simulate conditions within the body, such as body temperature and oxygen.

We have included this as a note. Here is the revision below:

“Note: It is recommended that the cells be placed in an environmental chamber to maintain heat, humidity, and CO₂ levels during image acquisition, as these parameters can influence cellular metabolism.”

13) Line 296, I would think the peak number of photons on the decay trace would depend on many things including the IRF. Does 100 photons really work as a minimum requirement for most systems?

Yes, the peak number of photons depends on many system variables including the IRF and number of time bins. We’ve added a note to the protocol to address this concern:

Note: The minimum peak number of photons within the fluorescence exponential decay is dependent on system parameters including temporal resolution, IRF, and background noise.

14) Line 300, why are four-five additional FOVs needed? Doesn't this number depend on the experimental design and effect size? This comment applies to other sections too.

This is recommended parameter that typically provides enough data at both the image and cell levels to resolve the expected changes with cyanide. However, the user can acquire more if so desired or complete a preliminary experiment for mean and standard deviation values to calculate the required n (number of images or number of cells) for a given experiment. These considerations have been added to the discussion.

“The protocol recommends 5-6 images of different fields of view be acquired from each experimental group as this sample size provides sufficient data at both the image and cell levels to resolve the expected differences in fluorescence lifetime parameters of confluent MCF7 cells due to the cyanide perturbation. The optimal number of images acquired per group depends on the experimental design and effect size.”

15) Are there any safety considerations for working with cyanide?

We thank the reviewer for bringing this to our attention. There are safety precautions when working with cyanide. We made to sure to add a caution notice when cyanide is first introduced in the protocol section of the paper. Here is the revision below:

“CAUTION: Cyanide is toxic. Wear appropriate personal protective equipment.”

16) Line 479, can the authors describe how to calculate an optical redox ratio? What software is used?

The redox ratio for fluorescence intensity imaging is calculated from the NAD(P)H and FAD intensity images through the formula $FAD / (FAD + NAD(P)H)$ computed at each pixel.

Image math can be performed in a variety of software packages including ImageJ/FIJI, CellProfiler, Matlab, or Python.

We have added a generalized protocol for the image analysis in the section titled “Fluorescence Intensity” in the protocol:

“

5.4. Image Level Redox Ratio Data Analysis

5.4.1. Open the NAD(P)H and FAD intensity images in an image processing program.

5.4.2. Set a threshold on the NAD(P)H to retain cytoplasm pixels and 0 background and nucleus pixels.

5.4.3. Calculate the redox ratio image by evaluating the equation $FAD / (NAD(P)H + FAD)$ at each pixel using the thresholded NAD(P)H image.

5.4.4. Calculate the mean value of the non-0 pixels.

Note: These steps can be performed in an image analysis software or coded directly with scripts.

5.5. Cell Level Redox Ratio Analysis

5.5.1. Follow Protocol Steps 4.3.1-4.3.12 to obtain a mask image of the cells within each NAD(P)H image.

5.5.2. Calculate the redox ratio image by evaluating the equation $FAD / (NAD(P)H + FAD)$ at each pixel.

5.5.3. Using the cell cytoplasm mask, average the redox ratio for all pixels for each cell within the image.

“



1 Alewife Center #200
Cambridge, MA 02140
tel. 617.945.9051
www.jove.com

VIDEO CONSENT AND RELEASE

Autofluorescence Imaging to Evaluate

Video (Working Title): Cellular Metabolism (the "Video")

Contributors: _____

Filming Date(s): _____

Filming Location(s): _____

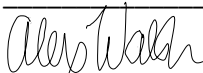
Producer: _JoVE

For a valuable consideration, including but not limited to filming, scripting and editing of the Video by Producer, receipt of which is hereby acknowledged, the undersigned Contributor hereby grants to Producer, its agents, employees, licensees, and successors in interest (collectively, the "Released Party") all ownership rights and the absolute and irrevocable right and permission to copyright, use and publish the Video, including without limitation the recorded names, likeness, image, voice, sound effects, interview and performance on the video, film, or otherwise (the "Recording"), edit such Recording as Producer may desire, and incorporate such Recording into the Video. For the avoidance of doubt, Producer shall retain final editorial, artistic, and technical control of the Video and the content of the Video. Producer may use, and authorize others to use, the Video, any portions thereof and the Recording in all markets, manner, formats and media, whether now known or hereafter developed, throughout the world, in perpetuity.

The Video may be copyrighted, used and/or published individually or in conjunction with other photography, video works, and recordings, and in any medium (including without limitation, print publications, public broadcast, CD-ROM format) and for any lawful purpose, including without limitation, trade, exhibition, illustration, promotion, publicity, advertising and electronic publication.

The undersigned represents and warrants that (i) no other party has been granted a license with respect to the Image and/or Voice, (ii) no other party's authorization or consent is required with respect to the permission granted to the Released Party under this Consent and Release, and (iii) the Contributor(s) listed at the top of this Video Release are the only contributors to this Video. The Contributor warrants that, if any Contributors' materials were used in production of this video, the use, reproduction, distribution, public or private performance or display, and/or modification of these materials does not and will not violate, infringe and/or misappropriate the patent, trademark, intellectual property or other rights of any third party. The Contributor represents and warrants that it has and will continue to comply with all government, institutional and other regulations, including, without limitation all institutional, laboratory, hospital, ethical, human and animal treatment, privacy, and all other rules, regulations, laws, procedures or guidelines, applicable to the Video, and that all research involving human and animal subjects has been approved by the Contributor's relevant institutional review board.

Name: Alex Walsh

Signature: 

Affiliation: TAMU

E-Mail: walshaj@tamu.edu

Date: 9/1/2021

For questions, please contact us at submissions@jove.com or +1.617.945.9051.

ARTICLE LICENSE AGREEMENT

Title of Article:

Autofluorescence Imaging to Evaluate Cellular Metabolism

Author(s):

Anna Theodossiou, Linghao Hu, Nianchao Wang, Uyen Nguyen,
Alex J. Walsh

Item 1: The Author elects to have the Article be made available (as described at <https://www.jove.com/authors/publication>) via:

☒

Standard Access



Open Access

Item 2: Please select one of the following items:

☒
The Author is **NOT** a United States government employee.

The Author is a United States government employee and the Article was prepared in the course of his or her duties as a United States government employee.

ARTICLE LICENSE AGREEMENT

1. **Defined Terms.** As used in this Article License Agreement, the following terms shall have the following meanings: **"Agreement"** means this Article License Agreement; **"Article"** means the manuscript submitted by Author(s) and specified on the last page of this Agreement, including texts, figures, tables and abstracts; **"Author"** means the author who is a signatory to this Agreement; **"Collective Work"** means a work, such as a periodical issue, anthology or encyclopedia, in which the Article, along with a number of other contributions, constituting separate and independent works in themselves, are assembled into a collective whole; **"CRC License"** means the Creative Commons Attribution-Non Commercial-No Derivs 3.0 Unported Agreement, the terms and conditions of which can be found at: <http://creativecommons.org/licenses/by-nc-nd/3.0/legalcode>; **"Derivative Work"** means a work based upon the Article and other pre-existing works, such as a translation, musical arrangement, dramatization, fictionalization, motion picture version, sound recording, art reproduction, abridgment, condensation, or any other form in which the Article may be recast, transformed, or adapted; **"Institution"** means the institution, listed on the last page of this Agreement, by which the Author was employed at the time of the creation of the Article; **"JoVE"** means MyJoVE Corporation, a Delaware corporation and the publisher of Journal of Visualized Experiments; **"Parties"** means the Author and JoVE.

2. **Background.** The Author, who is the author of the Article, in order to ensure the review, Internet formatting, publication, dissemination and protection of the Article, desires to have JoVE publish the Article. In furtherance of such goals, the Parties desire to

memorialize in this Agreement the respective rights of each Party in and to the Article.

3. **Grant of Rights in Article.** In consideration of JoVE agreeing to review, arrange and coordinate the peer review, format, publish and disseminate the Article, the Author hereby grants to JoVE, subject to **Sections 4 and 7** below, the exclusive, royalty-free, perpetual license (a) to publish, reproduce, distribute, display and store the Article in all forms, formats and media whether now known or hereafter developed (including without limitation in print, digital and electronic form) throughout the world, (b) to translate the Article into other languages, create adaptations, summaries or extracts of the Article or other Derivative Works or Collective Works based on all or any portion of the Article and exercise all of the rights set forth in (a) above in such translations, adaptations, summaries, extracts, Derivative Works or Collective Works and (c) to license others to do any or all of the above. The foregoing rights may be exercised in all media and formats, whether now known or hereafter devised, and include the right to make such modifications as are technically necessary to exercise the rights in other media and formats.

4. **Retention of Rights in Article.** The Author shall, with respect to the Article, retain the non-exclusive right to use all or part of the Article for the non-commercial purpose of giving lectures, presentations or teaching classes, and to post a copy of the Article on the Institution's website or the Author's personal website, in each case provided that a link to the Article on the JoVE website is provided and notice of JoVE's copyright in the Article is included. All non-copyright intellectual property rights in and to the Article, such as patent rights, shall remain with the Author.

5. Grant of Rights in Article – Standard Access. This

Section 5 applies if the “Standard Access” box has been checked in **Item 1** above or if no box has been checked in **Item 1** above. In consideration of JoVE agreeing to review, arrange and coordinate the peer review, format, publish and disseminate the Article, the Author hereby acknowledges and agrees that, Subject to **Section 7** below, JoVE is and shall be the sole and exclusive owner of all rights of any nature, including, without limitation, all copyrights, in and to the Article. To the extent that, by law, the Author is deemed, now or at any time in the future, to have any rights of any nature in or to the Article, the Author hereby disclaims all such rights and transfers all such rights to JoVE.

If the Author’s funding is a subject to the requirement of the NIH Public Access Policy, JoVE acknowledges that the Author retains the right to provide a copy of their final peer-reviewed manuscript to the NIH for archiving in PubMed Central 12 months after publication by JoVE.

Notwithstanding anything else in this agreement, if the Author’s funding is a subject to the requirements of Plan S, JoVE acknowledges that the Author retains the right to provide a copy of the Author’s accepted manuscript for archiving in a Plan S approved repository under a Plan S approved license.

6. Grant of Rights in Article – Open Access. This

Section 6 applies only if the “Open Access” box has been checked in **Item 1** above. JoVE and the Author hereby grant to the public all such rights in the Article as provided in, but subject to all limitations and requirements set forth in, the CRC License.

7. USA Government Employees. If the Author is a United States government employee and the Article was prepared in the course of his or her duties as a United States government employee, as indicated in **Item 2** above, and any of the licenses or grants granted by the Author hereunder exceed the scope of the 17 U.S.C. 403, then the rights granted hereunder shall be limited to the maximum rights permitted under such statute. In such case, all provisions contained herein that are not in conflict with such statute shall remain in full force and effect, and all provisions contained herein that do so conflict shall be deemed to be amended so as to provide to JoVE the maximum rights permissible within such statute.

8. Protection of the Work. The Author(s) authorize JoVE to take steps in the Author(s) name and on their behalf if JoVE believes some third party could be infringing or might infringe the copyright of the Article.

9. Privacy, Personality. The Author hereby grants JoVE the right to use the Author’s name, picture, photograph, image, biography, likeness, voice and performance in any way, commercial or otherwise, in connection with the Articles and the sale, promotion and distribution thereof.

10. Author Warranties. The Author represents and warrants that the Article is original, that it has not been published, that the copyright interest is owned by the Author (or, if more than one author is listed at the

beginning of this Agreement, by such authors collectively) and has not been assigned, licensed, or otherwise transferred to any other party. The Author represents and warrants that the author(s) listed at the top of this Agreement are the only authors of the Article. If more than one author is listed at the top of this Agreement and if any such author has not entered into a separate Article License Agreement with JoVE relating to the Article, the Author represents and warrants that the Author has been authorized by each of the other such authors to execute this Agreement on his or her behalf and to bind him or her with respect to the terms of this Agreement as if each of them had been a party hereto as an Author. The Author warrants that the use, reproduction, distribution, public or private performance or display, and/or modification of all or any portion of the Article does not and will not violate, infringe and/or misappropriate the patent, trademark, intellectual property or other rights of any third party. The Author represents and warrants that it has and will continue to comply with all government, institutional and other regulations, including, without limitation all institutional, laboratory, hospital, ethical, human and animal treatment, privacy, and all other rules, regulations, laws, procedures or guidelines, applicable to the Article, and that all research involving human and animal subjects has been approved by the Author’s relevant institutional review board.

11. JoVE Discretion. If more than one author is listed at the beginning of this Agreement, JoVE may, in its sole discretion, elect not take any action with respect to the Article until such time as it has received complete, executed Article License Agreements from each such author. JoVE reserves the right, in its absolute and sole discretion and without giving any reason therefore, to accept or decline any work submitted to JoVE. JoVE has sole discretion as to the method of reviewing, formatting and publishing the Article, including, without limitation, all decisions regarding timing of publication, if any.

12. Indemnification. The Author agrees to indemnify JoVE and/or its successors and assigns from and against any and all claims, costs, and expenses, including attorney’s fees, arising out of any breach of any warranty or other representations contained herein. The Author further agrees to indemnify and hold harmless JoVE from and against any and all claims, costs, and expenses, including attorney’s fees, resulting from the breach by the Author of any representation or warranty contained herein or from allegations or instances of violation of intellectual property rights, damage to the Author’s or the Author’s institution’s facilities, fraud, libel, defamation, research, equipment, experiments, property damage, personal injury, violations of institutional, laboratory, hospital, ethical, human and animal treatment, privacy or other rules, regulations, laws, procedures or guidelines, liabilities and other losses or damages related in any way to the submission of work to JoVE, or publication in JoVE or elsewhere by JoVE. All indemnifications provided herein shall include JoVE’s attorney’s fees and costs related to said

ARTICLE LICENSE AGREEMENT


losses or damages. Such indemnification and holding harmless shall include such losses or damages incurred by, or in connection with, acts or omissions of JoVE, its employees, agents or independent contractors.

13. **Fees.** To cover the cost incurred for its work, JoVE must receive payment before publication of the Article. Payment is due 21 days after invoice. Should the Articles not be published due to the JoVE's decision, these funds will be returned to the Author. If payment is not received before the publication of the Article, the publication will be suspended until payment is received.

14. **Transfer, Governing Law.** This Agreement may be assigned by JoVE and shall inure to the benefits of any of

JoVE's successors and assignees. This Agreement shall be governed and construed by the internal laws of the Commonwealth of Massachusetts without giving effect to any conflict of law provision thereunder. This Agreement may be executed in counterparts, each of which shall be deemed an original, but all of which together shall be deemed to be one and the same agreement. A signed copy of this Agreement delivered by facsimile, e-mail or other means of electronic transmission shall be deemed to have the same legal effect as delivery of an original signed copy of this Agreement.

CORRESPONDING AUTHOR

Name:	Alex J. Walsh	
Department:	Biomedical Engineering	
Institution:	Texas A&M University-College Station	
Title:	Assistant Professor	
Signature:		Date: 9/1/2021

Please submit a **signed** and **dated** copy of this license by one of the following three methods:

1. Upload an electronic version on the JoVE submission site
2. Email the document to submissions@jove.com
3. Fax the document to +1.866.381.2236
4. Mail the document to JoVE / Attn: JoVE Editorial / 1 Alewife Center #200 / Cambridge, MA 02140